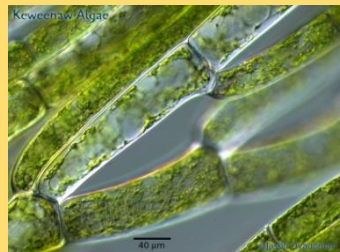
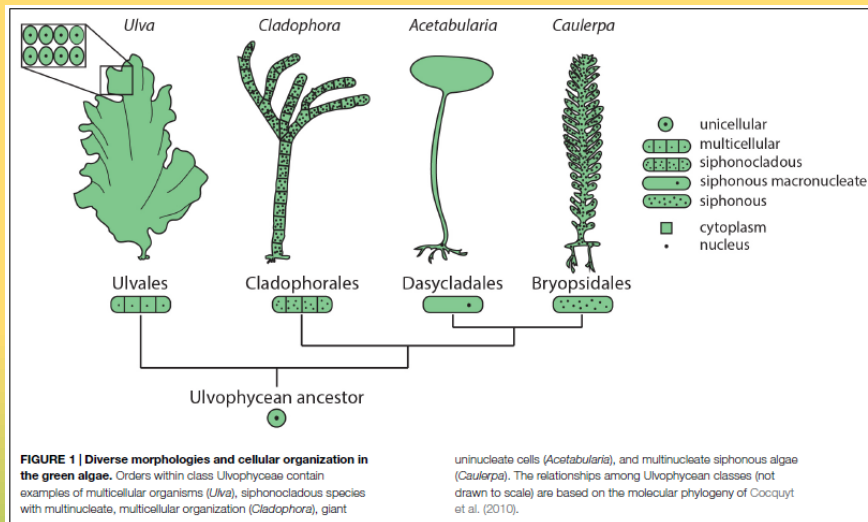


Ulvophyceae - Cladophorales



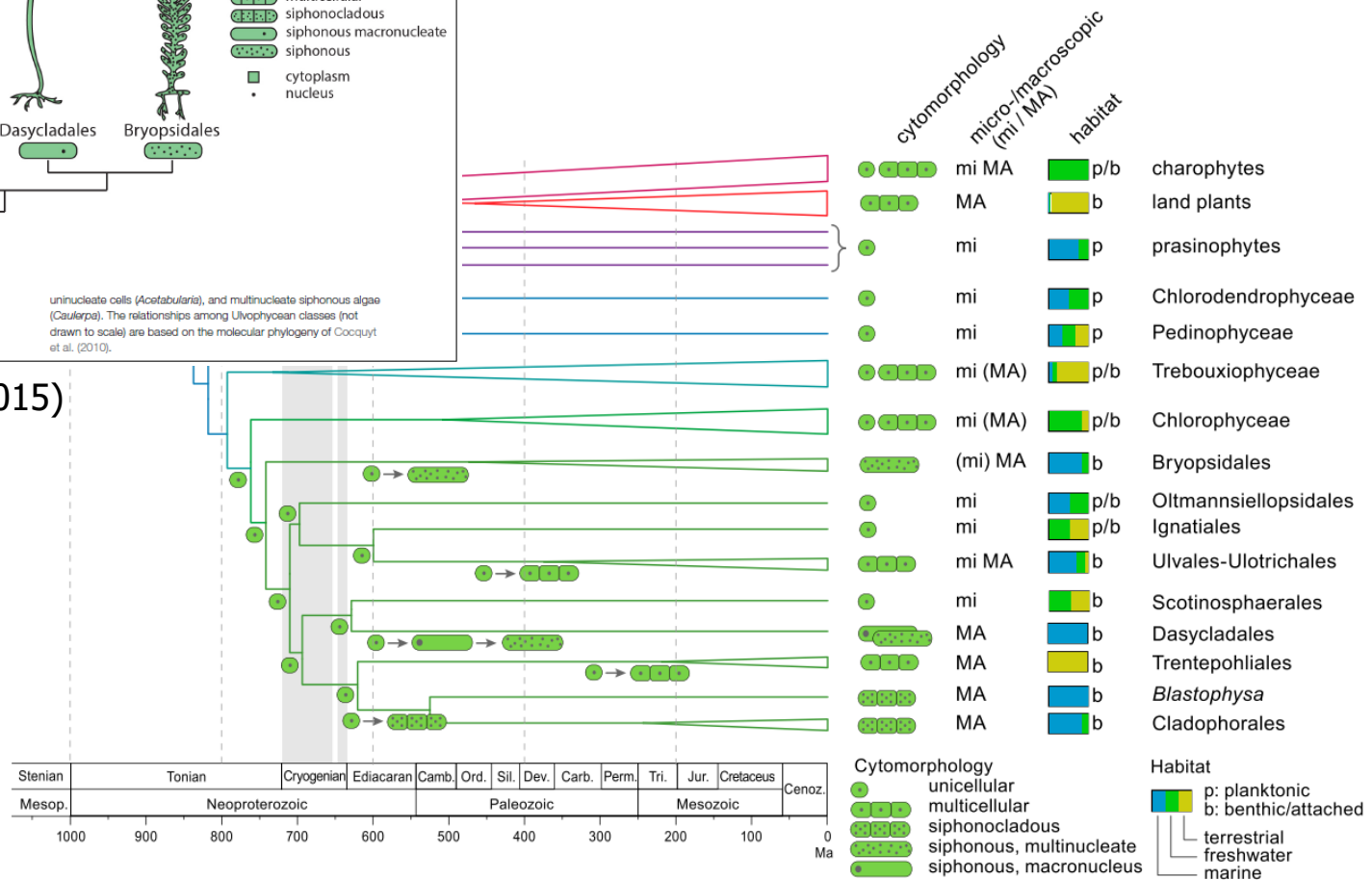
Základní charakteristika

Sifonokladální stélka



Del Cortona et al. (2020)

Coneva & Chitwood (2015)



Cockquyt et al. (2010)

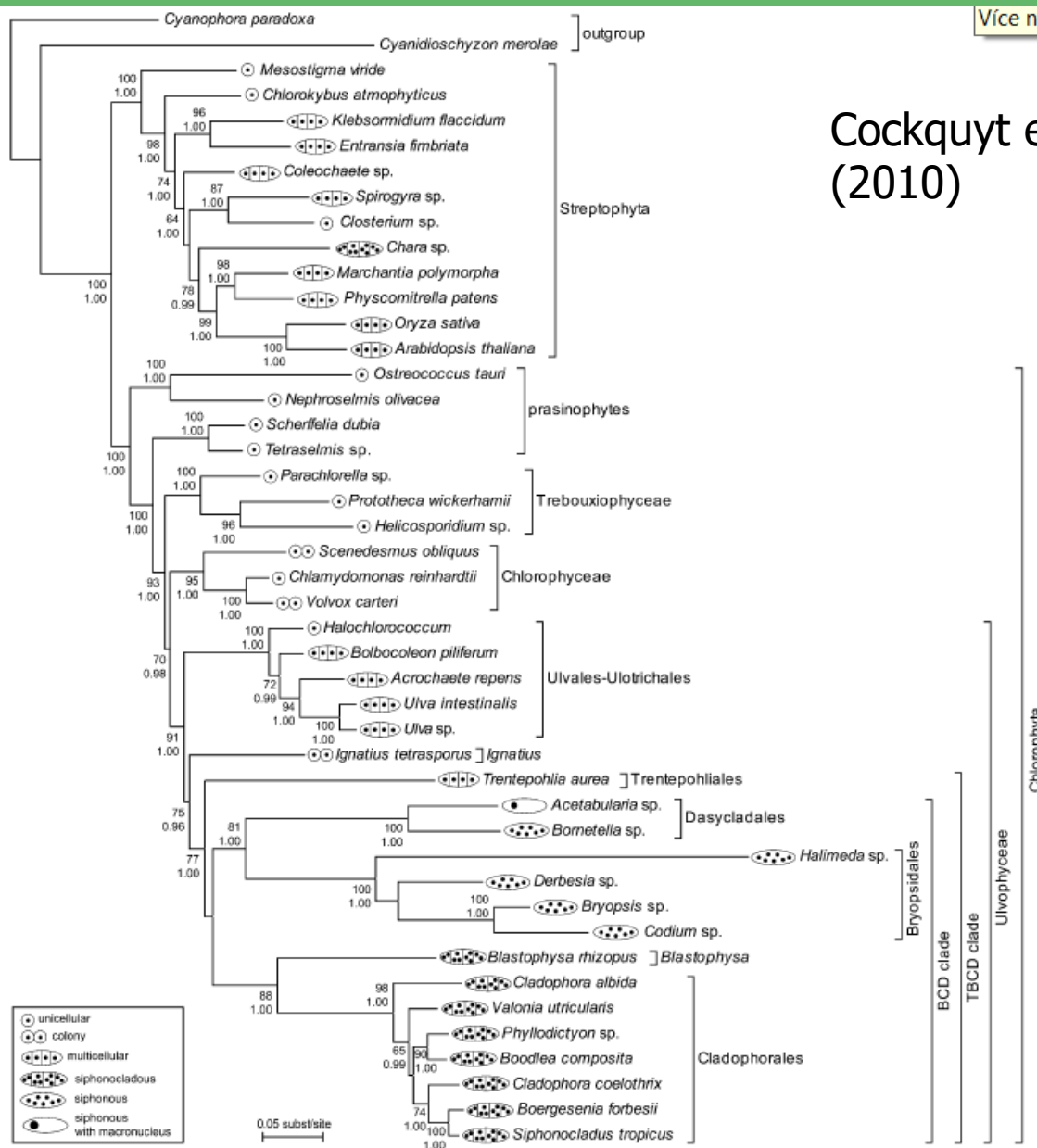
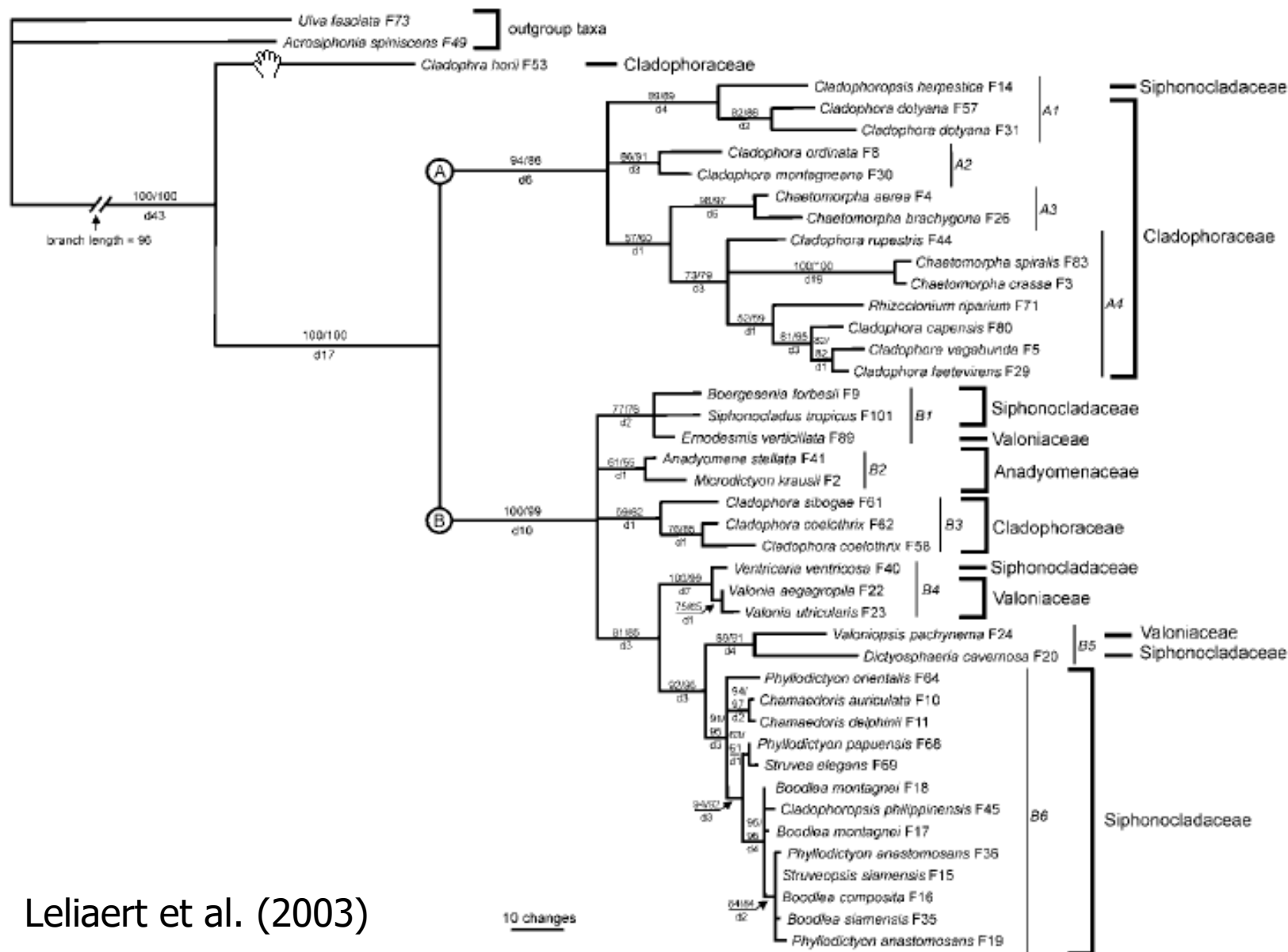


FIG. 1. Phylogeny of the green plant lineage obtained by ML inference of the 25% site-stripped data set containing seven nuclear genes, SSU nrDNA, and plastid genes *rbcL* and *atpB*. Numbers at nodes indicate ML BVs (top) and BI PP (bottom); values below, respectively, 50 and 0.9 are not shown. BCD clade stands for the orders Bryopsidales, Cladophorales, and Dasycladales, and TBCD clade stands for the orders Trentepohliales, Bryopsidales, Cladophorales, and Dasycladales.

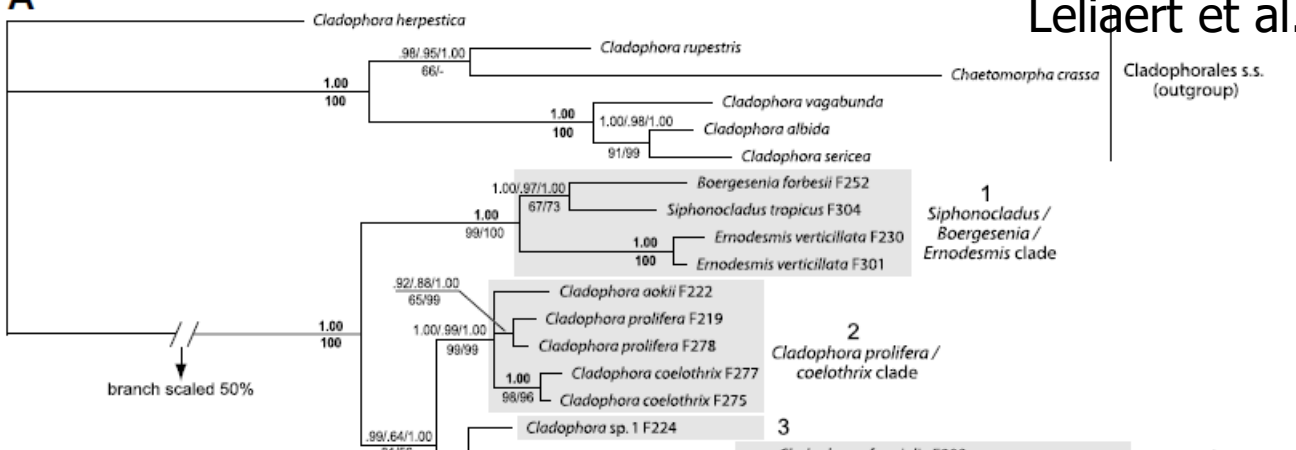
Evoluce



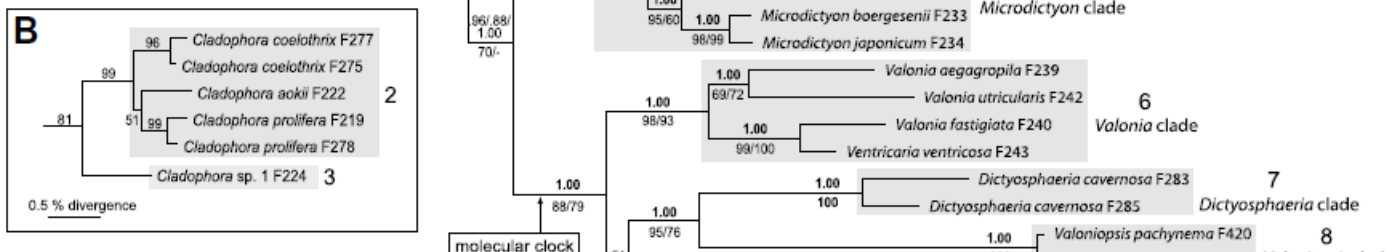
Evolute

Leliaert et al. (2007)

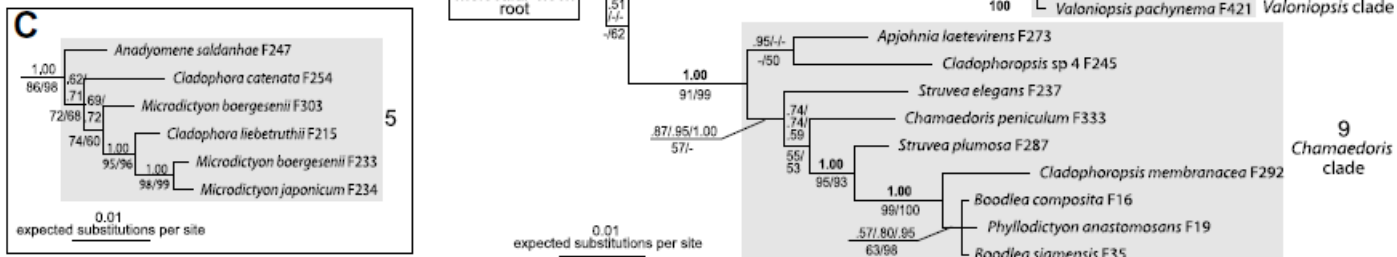
A



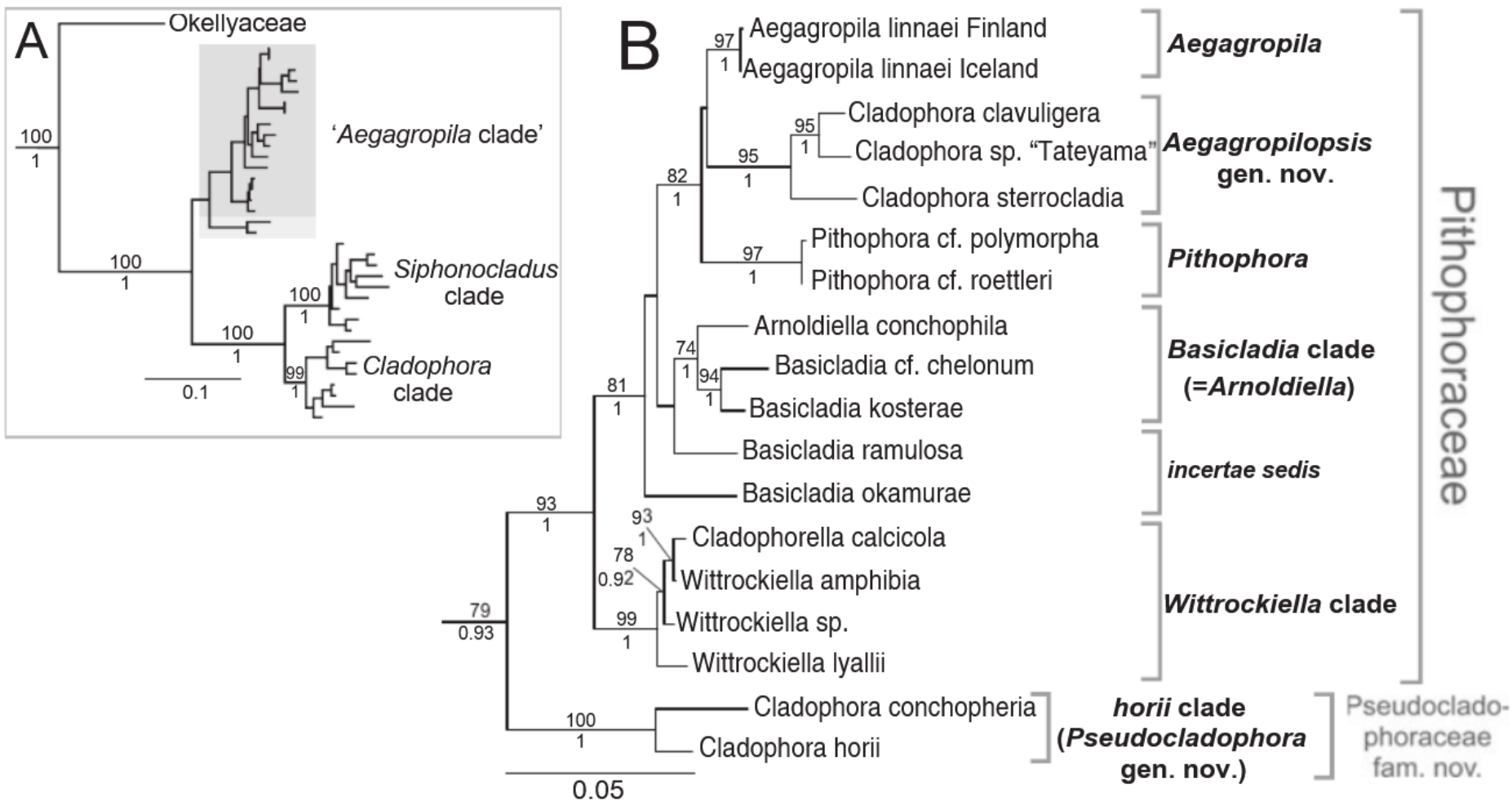
B



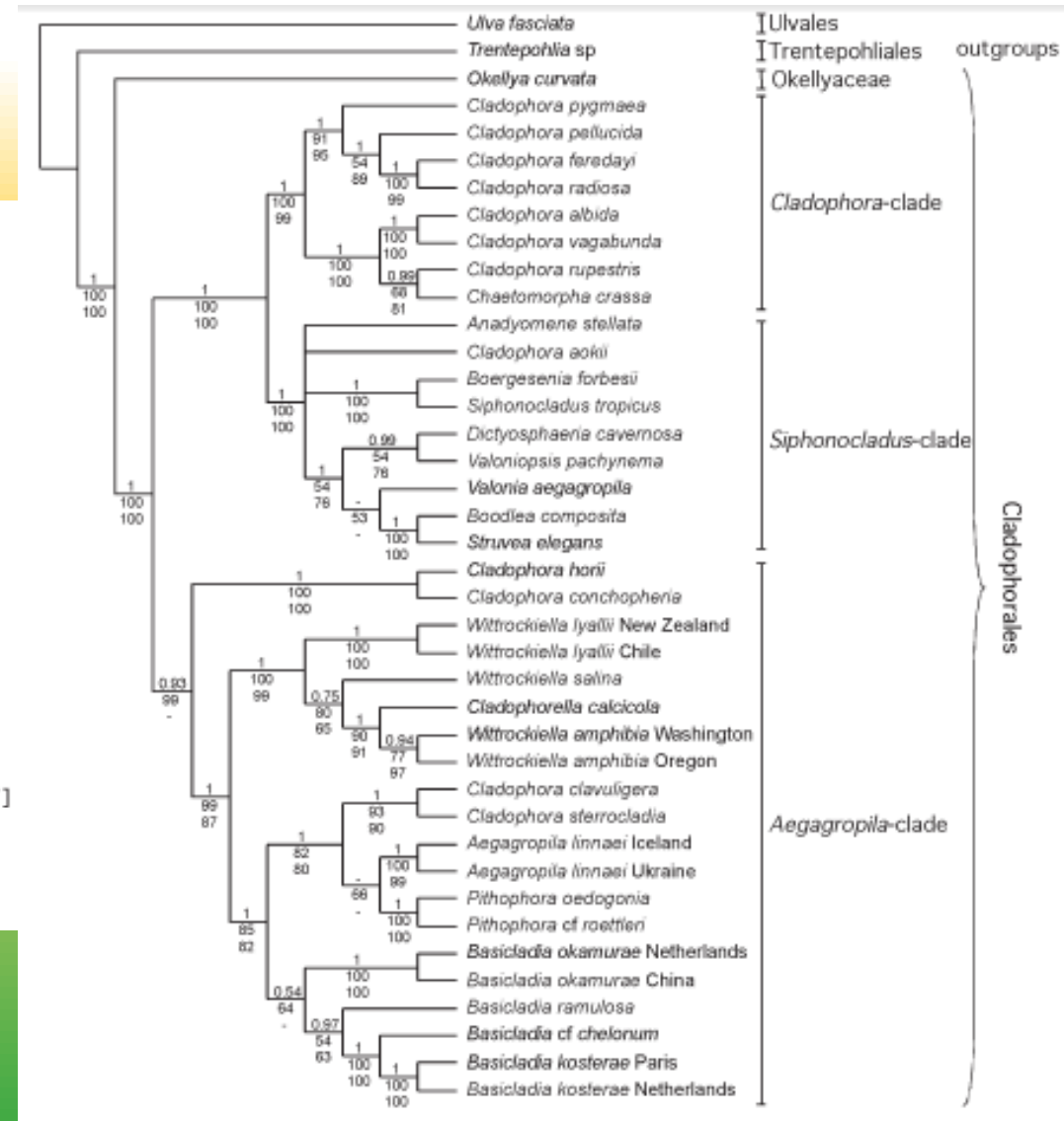
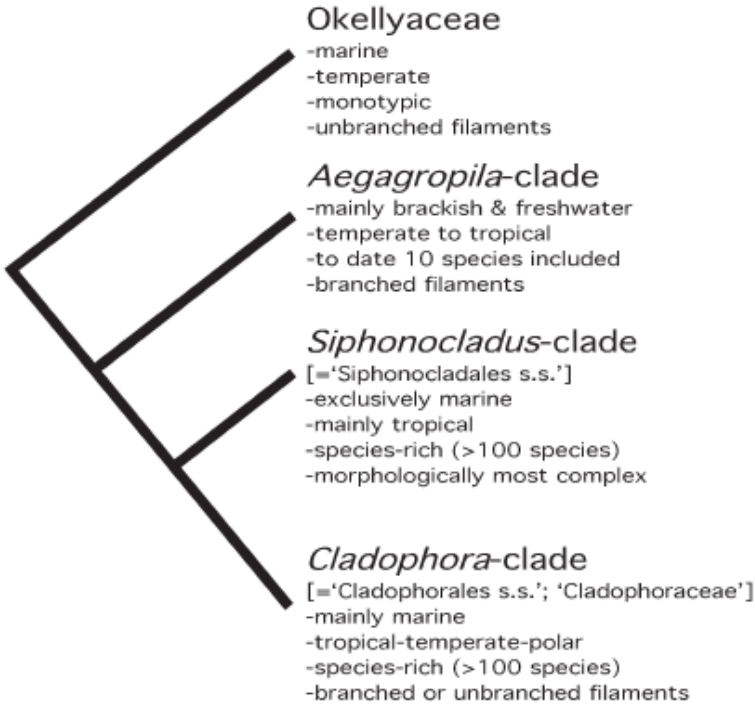
C



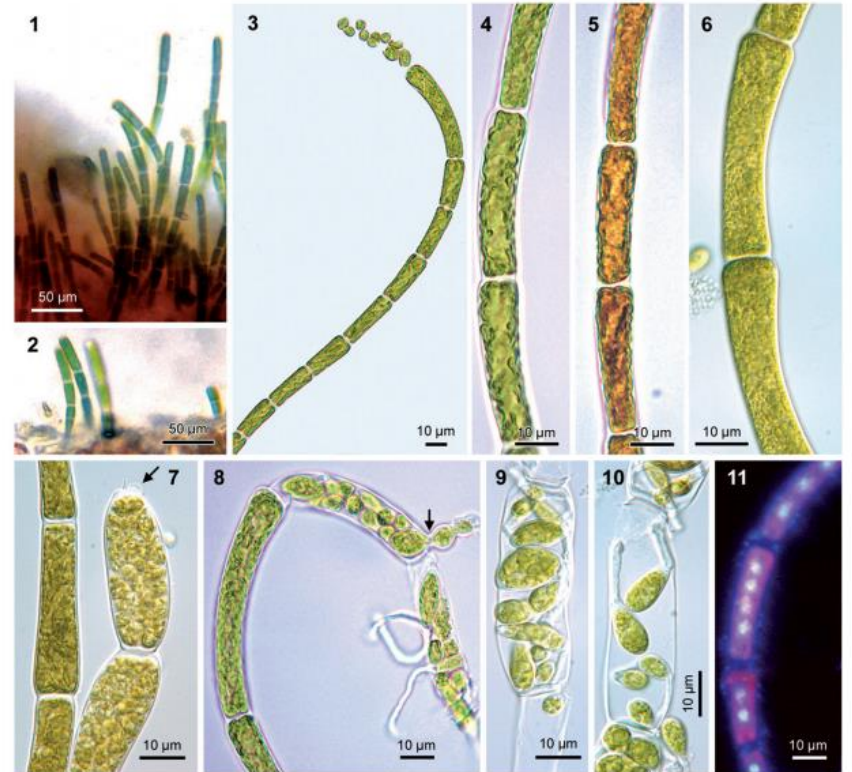
Evolute



Systém



Cladophorales – *Okellya* clade



Figs 1–11. *Uronema curvatum* (=*Okellya curvata*, comb. nov.). Figs 1, 2. Field-collected sample, growing as an epiphyte on a red crust, on the haptera of *Laminaria hyperborea* (diameter of filaments 7–8 µm). Figs 3–11. Cultures. Fig. 3. Terminal sporangia with spores. Figs 4, 5. Vegetative filaments showing chloroplasts before and after staining with iodine solution (no pyrenoids are visible). Fig. 6. Irregular surface of chloroplast. Figs 7–10. Terminal sporangia with spores, some of which germinate *in situ*. Arrows indicate exit pore. Fig. 11. DAPI-stained vegetative cells with two to four nuclei.

Okellya curvata

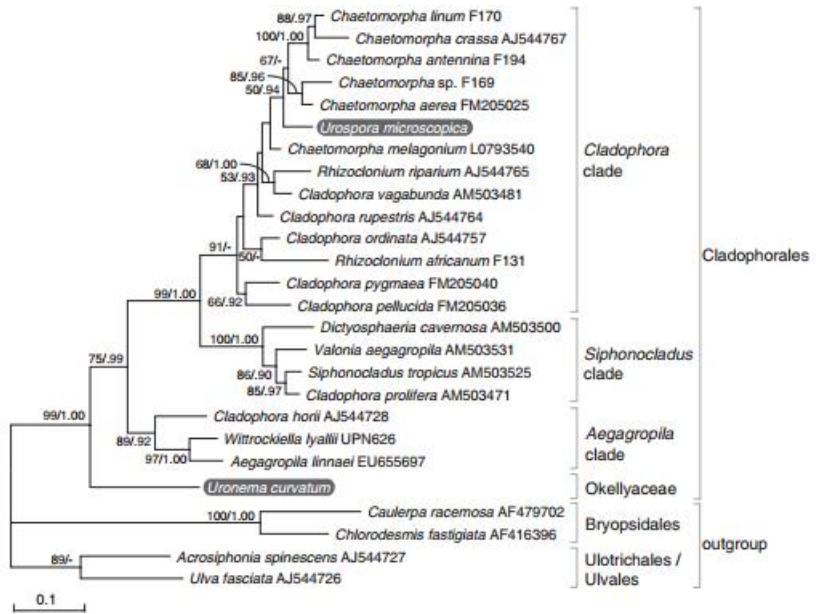


Fig. 23. Maximum likelihood (ML) tree of the Cladophorales inferred from partial large subunit nrDNA sequences, showing the phylogenetic position of *Uronema curvatum* (=*Okellya curvata*, comb. nov.) and *Urospora microscopica* (=*Chaetomorpha norvegica*, nom. nov.). ML bootstrap values (> 50) and Bayesian inference posterior probabilities (> 0.90) are indicated at branches.

Cladophorales – *Cladophora* clade

Boedecker et al. (2016)

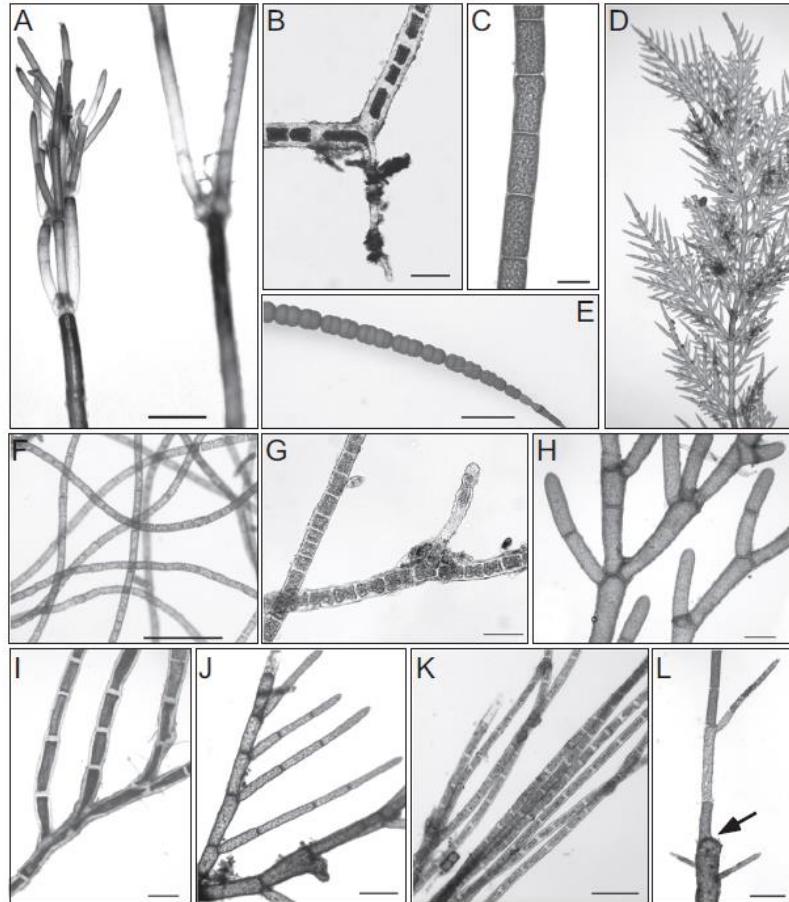
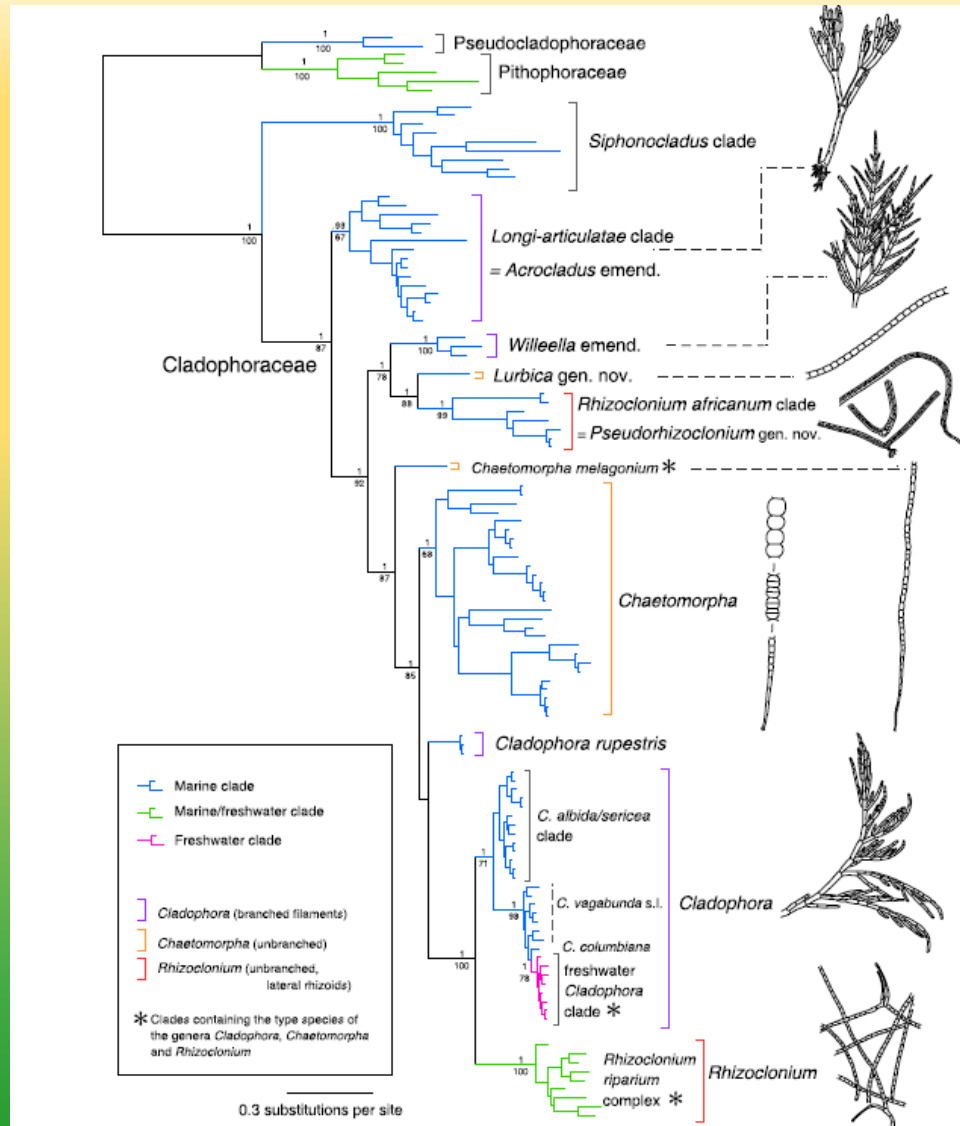
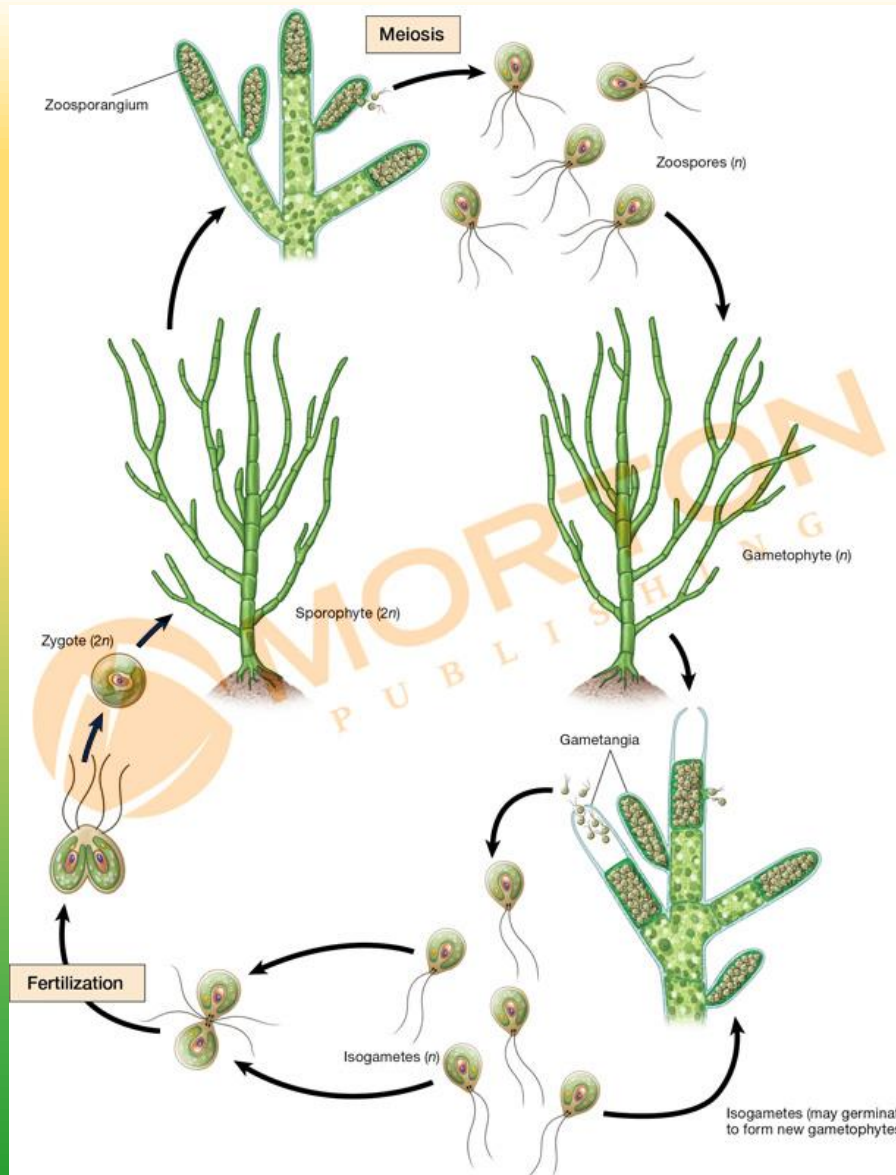


FIG. 1. Morphological diversity within the Cladophoraceae. (A) *Cladophora pellucida* (= *Acrocladus pellucidus*), apical part of thallus showing dense acropetal branching and long cells in main filaments, scale bar = 1 mm. (B) *Rhizoclonium africanum* (= *Pseudorhizoclonium africanum* comb. nov.), unbranched filaments with lateral rhizoid showing characteristic thick cell walls, field material, scale bar = 100 µm. (C) *Rhizoclonium africanum* (= *Pseudorhizoclonium africanum* comb. nov.), culture of field material shown in (B), unbranched filament with thin cell walls, scale bar = 100 µm. (D) *Cladophora ordinata* (= *Willella ordinata*), upper part of thallus showing characteristic opposite branching, scale bar = 500 µm. (E) *Chaetomorpha cf. formis*, basal region of unbranched filament showing the characteristic giant cells organized in pairs, scale bar = 5 mm. (F) *Chaetomorpha ligata*, thin unbranched filaments, scale bar = 500 µm. (G) *Rhizoclonium "riparium"*, unbranched filaments with lateral rhizoids, scale bar = 50 µm. (H) *Cladophora leptostroma*, branched thallus, scale bar = 200 µm. (I) *Cladophora glomerata*, basal part of thallus with thick cell walls and irregular insertion of branches, scale bar = 200 µm. (J) *Cladophora glomerata*, densely branched apical part of thallus showing acropetal growth, scale bar = 100 µm. (K) *Cladophora cf. fracta*, unbranched filaments, scale bar = 100 µm. (L) *Cladophora rivulans*, variability in culture, with drastically reduced filament width in culture (arrow indicates transition) compared to thicker diameter as encountered in the field, scale bar = 50 µm.



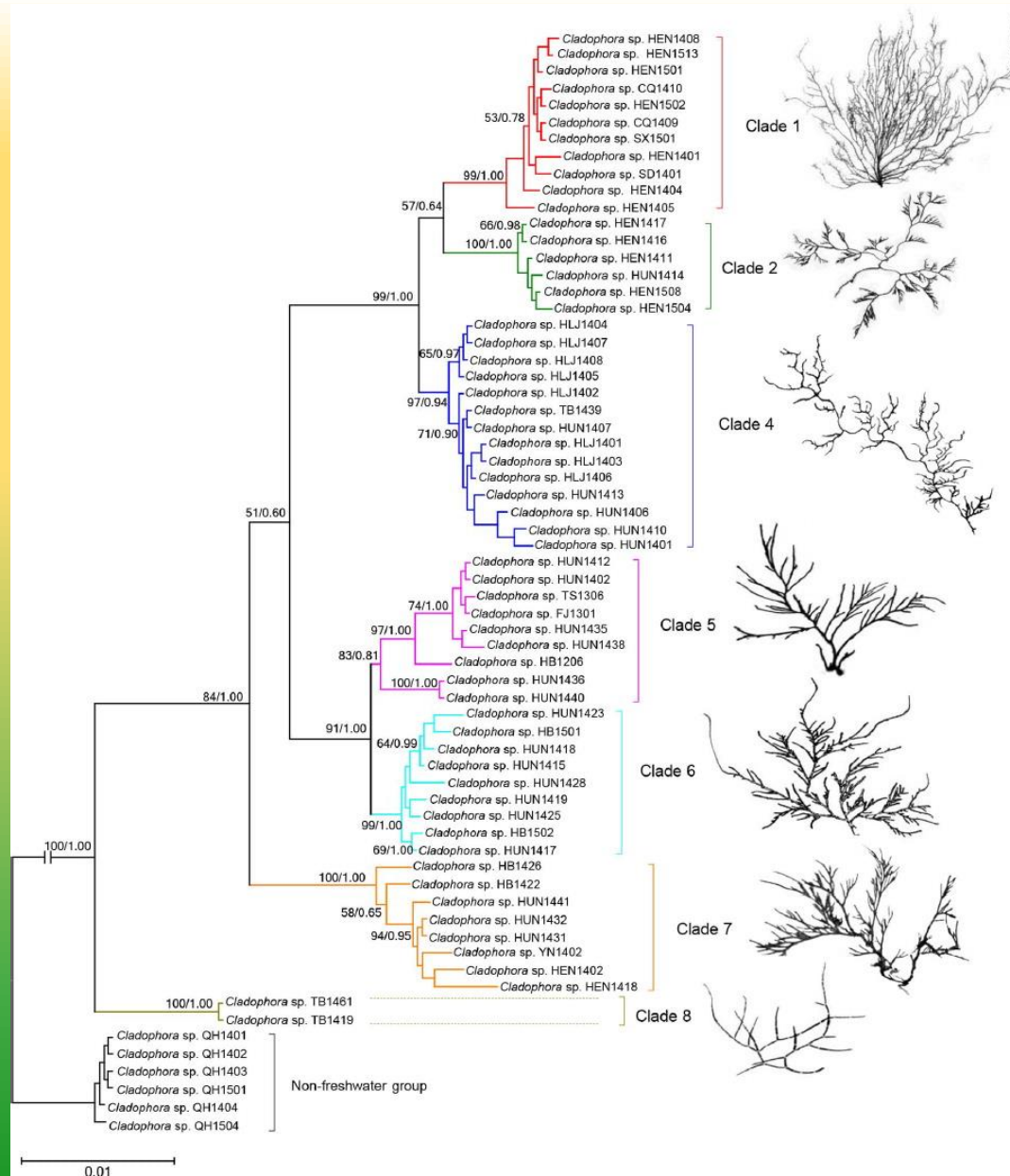
Cladophorales – *Cladophora* clade



Graham et al. (2016)

Cladophorales – *Cladophora* clade

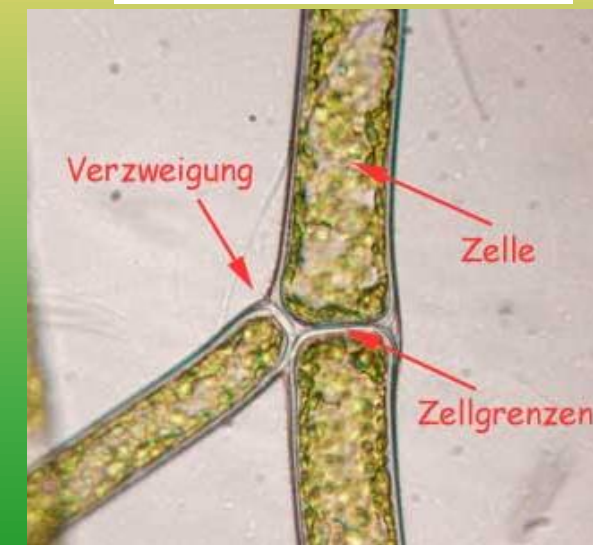
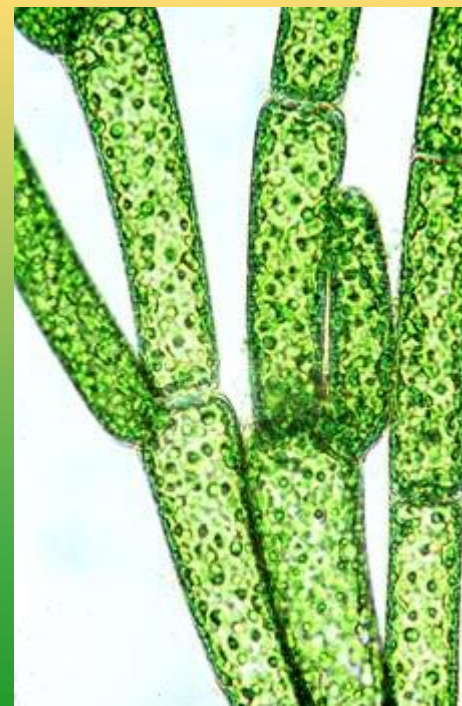
Cladophora



Zhu et al. (2019)

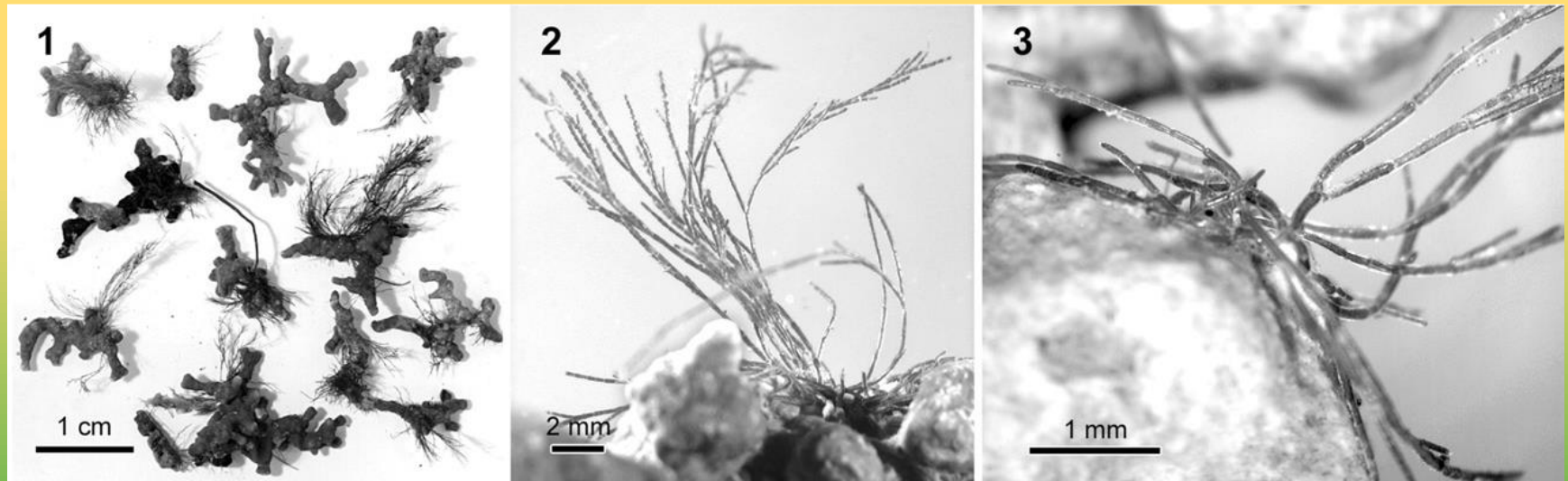
Cladophorales – *Cladophora* clade

Cladophora



Cladophorales – *Cladophora* clade

Cladophora rhodolithicola



Leliaert et al. (2009)

***Cladophora* – význam:**

- Hnojivo, krmivo
- Látky pro farmaceutický průmysl a kosmetiku
- Stavebnictví (polyuretanové pěny)
- fytoremediace
- Potravina – v Thajsku „kaï“
- Řada studií ohledně potenciálního antioxidačního, antibakteriálního a antirakovinného účinku nebo využití pro biofuels
- „habitat forming species“ v estuáriích, řekách apod.



Zulkifly et al. (2013)

Cladophorales – *Cladophora* clade

Rhizoclonium

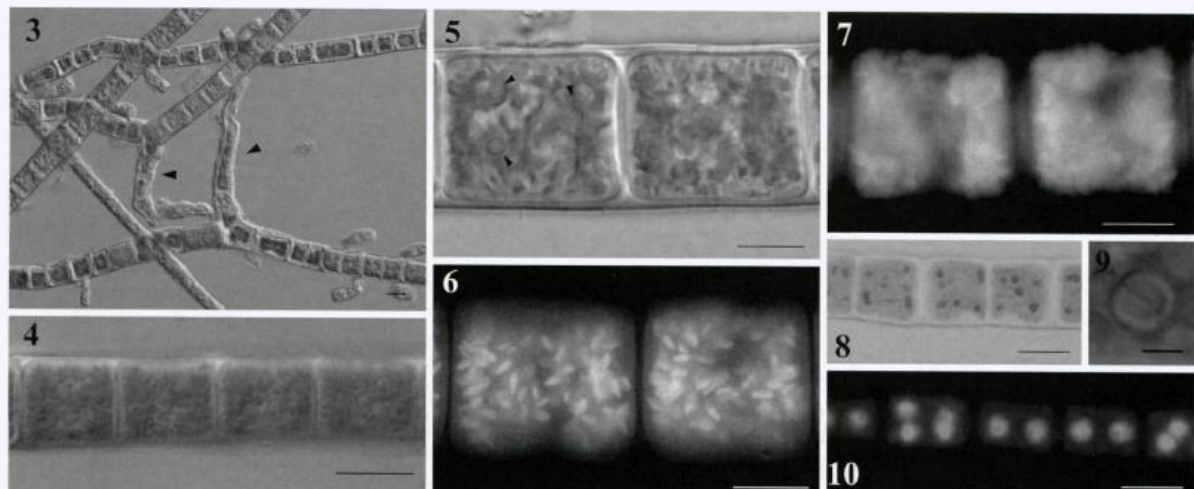


Fig. 3. Field collected material showing filaments that form rhizoids (arrowheads).

Figs 4, 5. Reticulate chloroplasts. Arrowheads indicate pyrenoids.

Figs 6, 7. Autofluorescent chloroplasts. Some chloroplasts are arranged in a reticulate pattern.

Fig. 8. Cells stained with Lugol's iodine, showing the pyrenoids.

Fig. 9. Bilenticular pyrenoid.

Fig. 10. Cells stained with DAPI, showing nuclei.

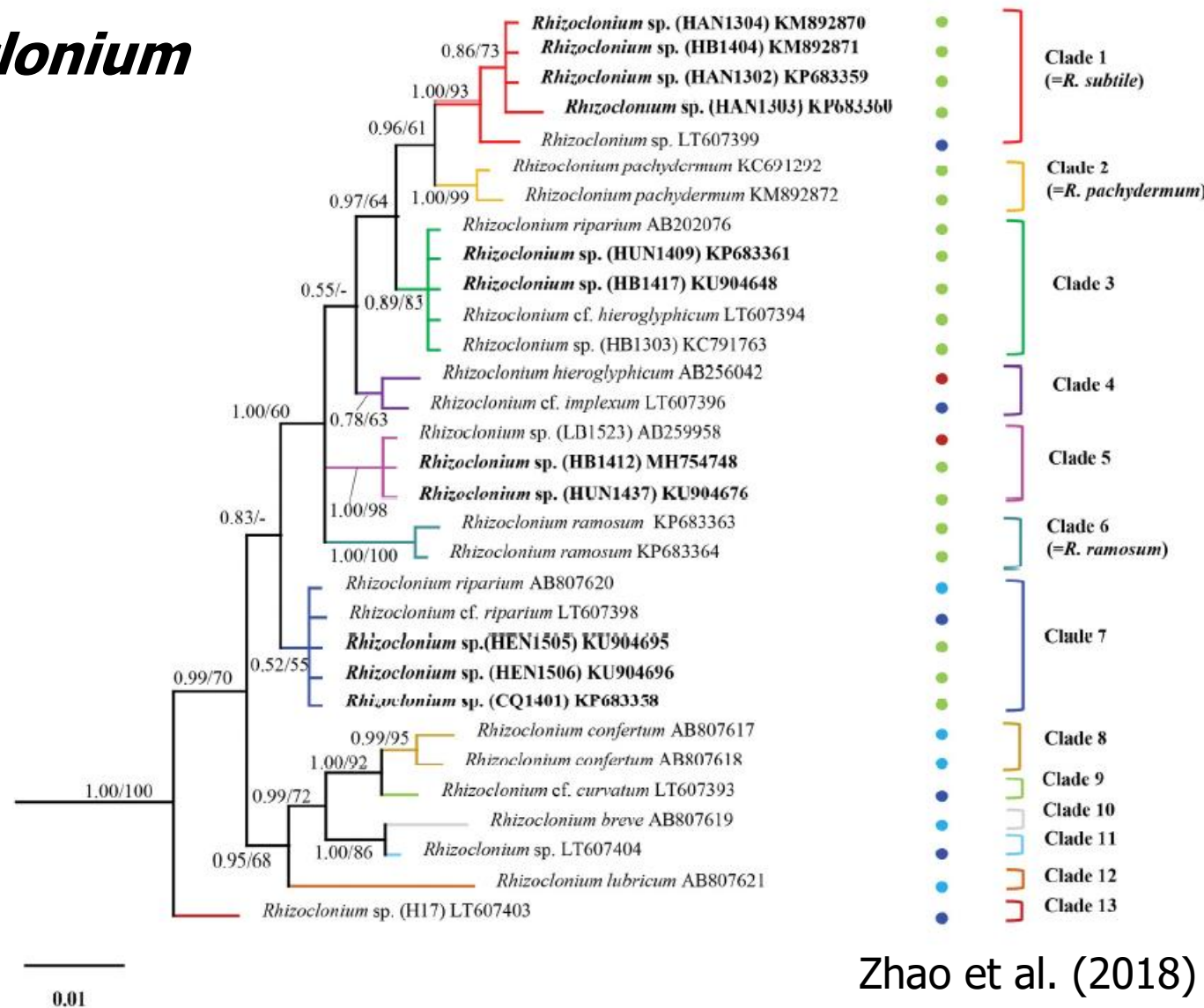
Ichihara et al. (2013)



algaeBASE

Cladophorales – *Cladophora* clade

Rhizoclonium



Zhao et al. (2018)

Cladophorales – *Cladophora* clade

Chaetomorpha

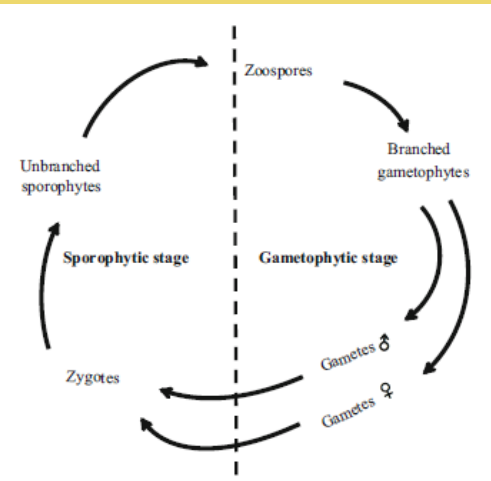
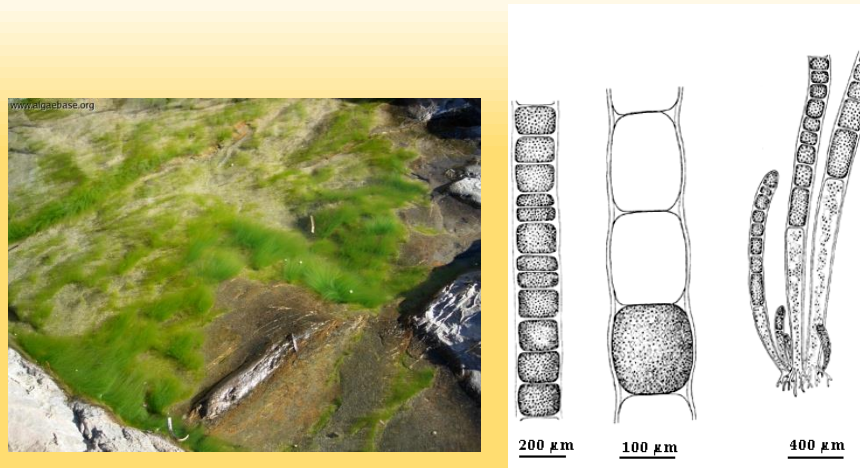


Fig.5 The heteromorphic life cycle of *Chaetomorpha valida* in culture

Male and female gametes discharged from gametophytes fused into zygotes. Zygotes settled and developed into unbranched sprophytes, which then released zoospores. Zoospores germinated and developed into new branched gametophytes to complete the life cycle.

Deng et al. (2013)

Cladophorales *Siphonocladus* clade

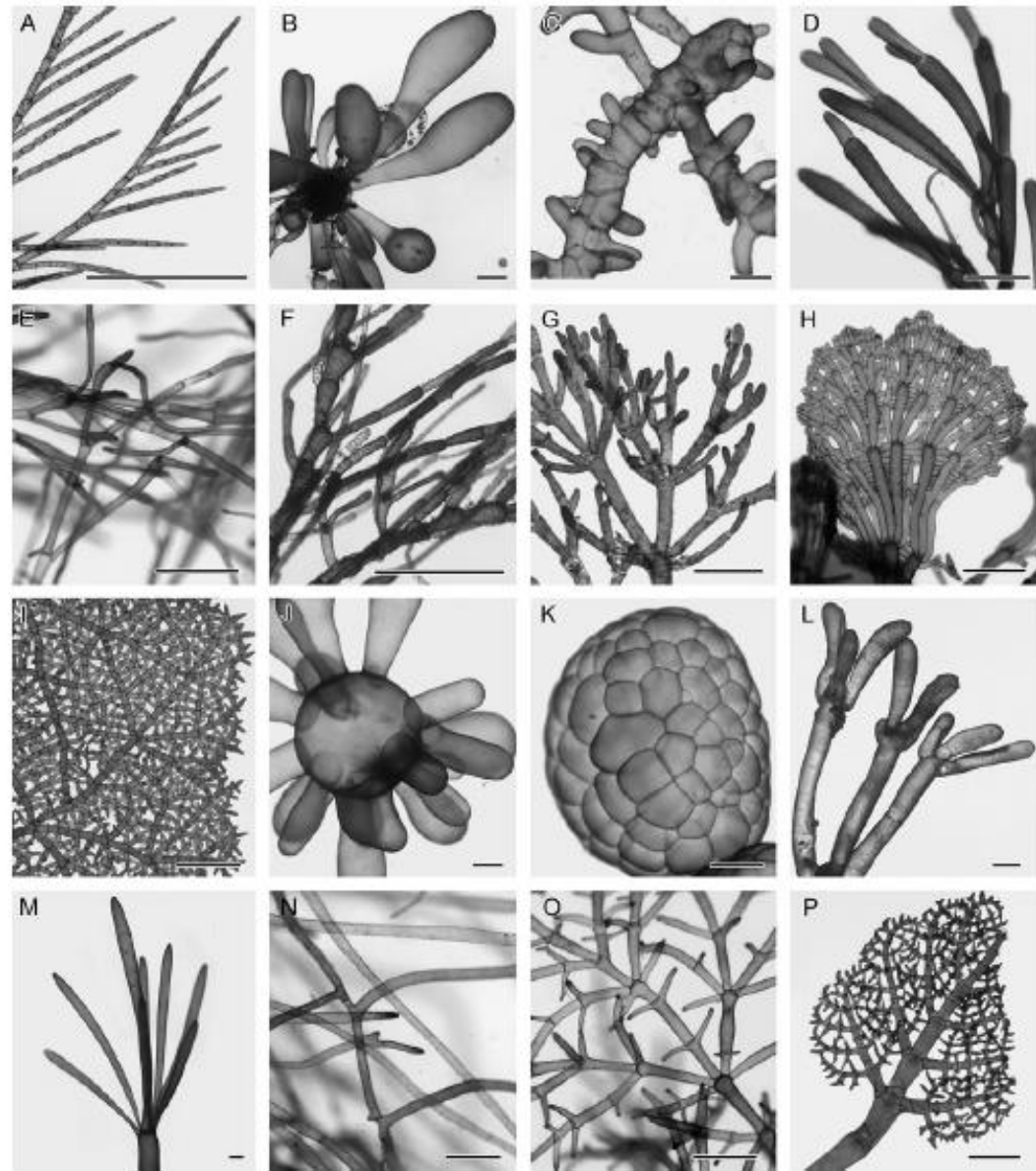
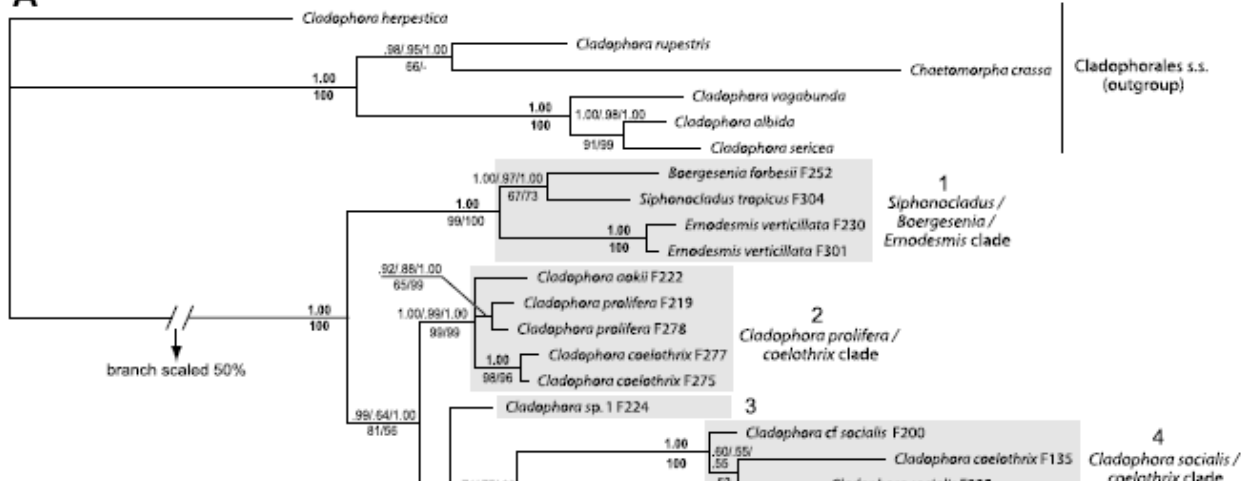


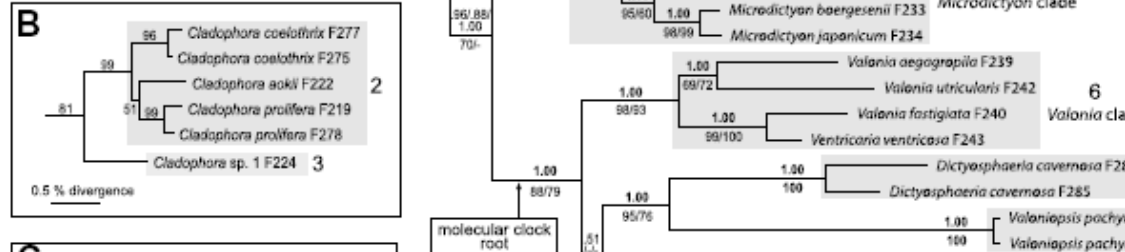
Fig. 1. Morphological variety in the Siphonocladales (A) *Cladophora sericea* (Cladophorales; outgroup), (B) *Boergesenia forbesii* (F252; clade 1), (C) *Siphonocladus pusillus* (F306; clade 1), (D) *Cladophora prolifera* (F280; grade 2), (E) *Cladophora coelothrix* (F275; grade 2), (F) *Cladophora* sp. 1 (F224; "clade" 3), (G) *Cladophora sibogae* (F61; clade 4), (H) *Anadyomene stellata* (F268, clade 5), (I) *Microdictyon krausii* (F2; clade 5), (J) *Valonia utricularis* (F242; clade 6), (K) *Dictyosphaeria cavemosa* (F283; clade 7), (L) *Valonopsis pachynema* (F24; clade 8), (M) *Apjohnia kuetevirens* (F273; clade 9), (N) *Cladophoropsis membranacea* (F295; clade 9), (O) *Phyllodictyon orientale* (F414; clade 9), (P) *Phyllodictyon anastomosans* (F36; clade 9). Scale bars, 1 mm.

Cladophorales - *Siphonocladus* clade

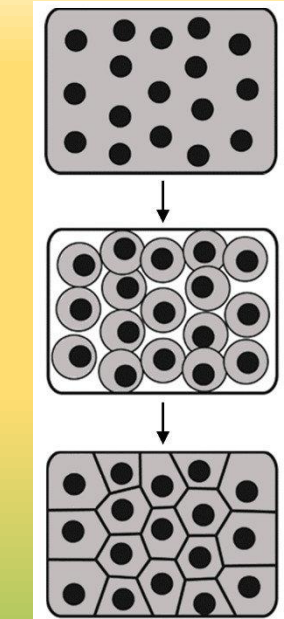
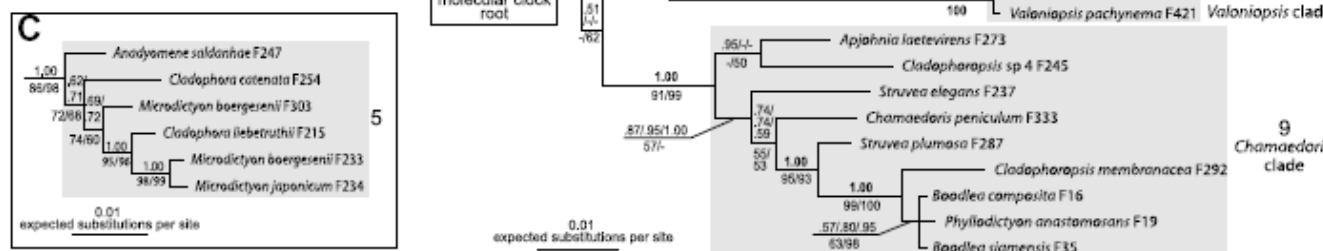
A



B



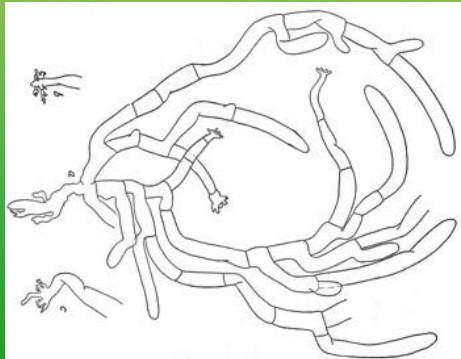
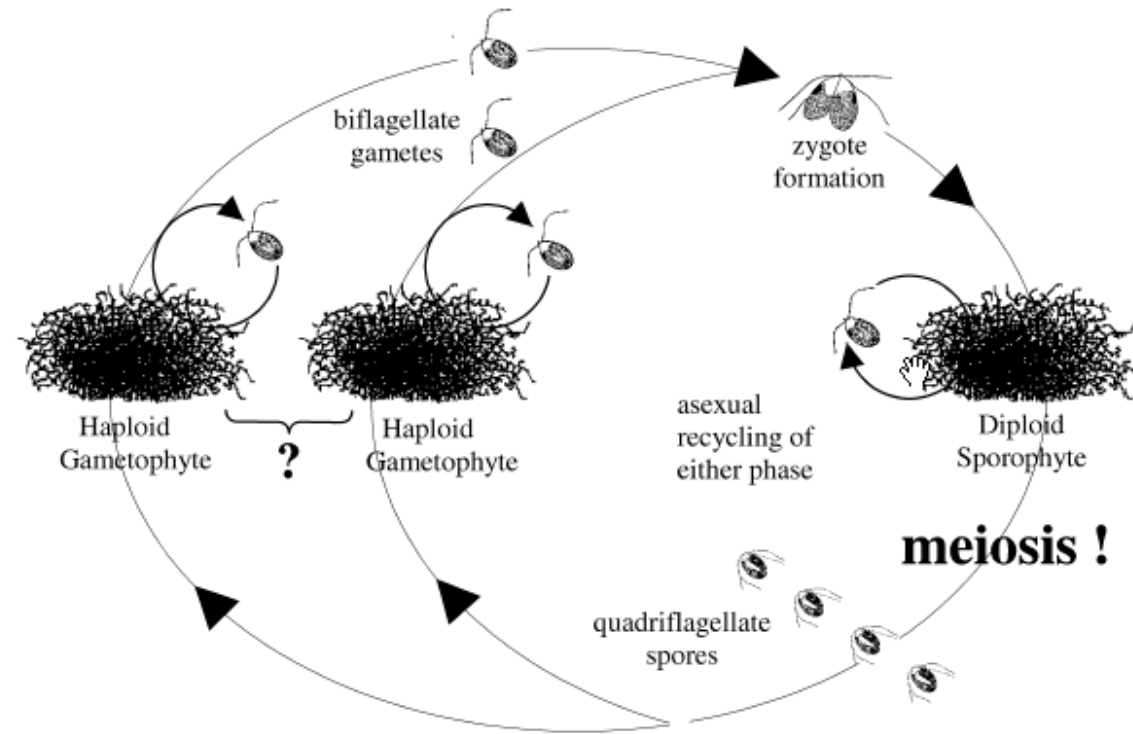
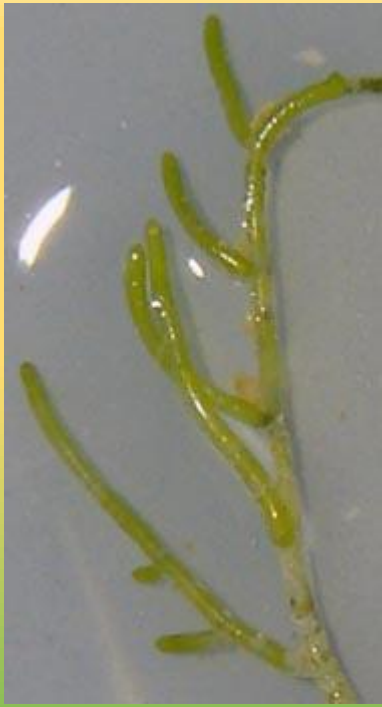
C



**Segregative
cell division**

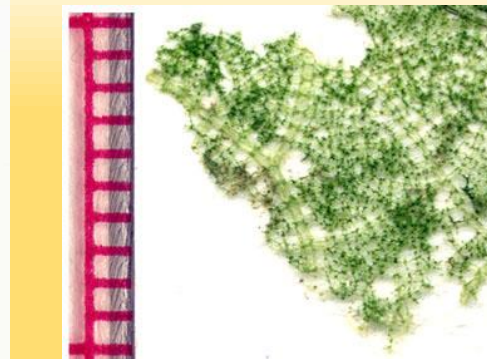
Cladophorales - *Siphonocladus* clade

Cladophoropsis



Cladophorales - *Siphonocladus* clade

Microdictyon



A.W. Bruckner, 2002

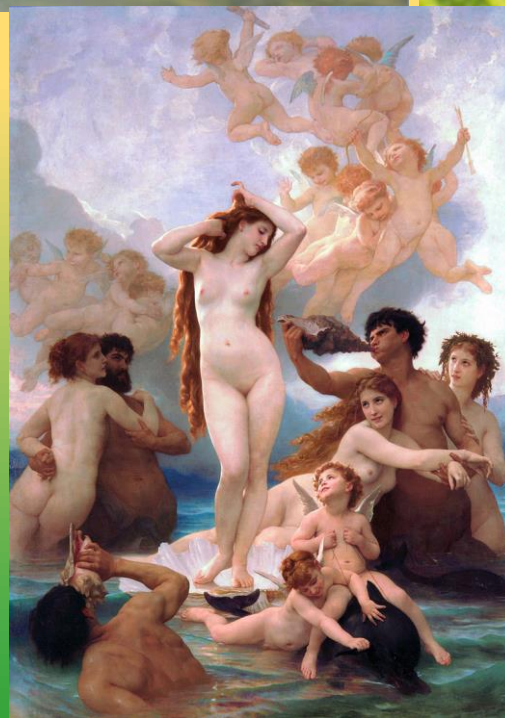
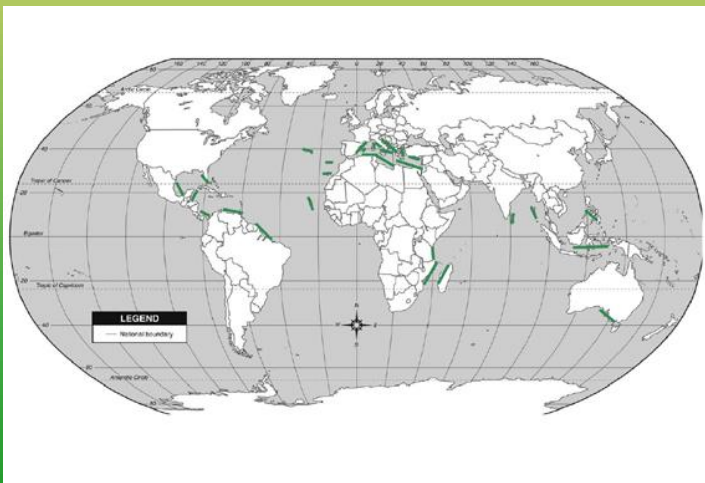


Cladophorales - *Siphonocladus* clade

Anadyomene



A. stellata – mediterán



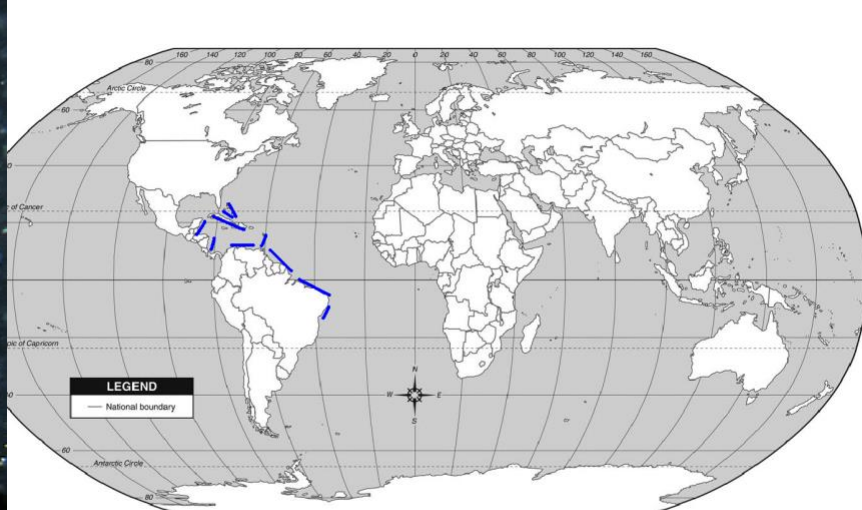
Bouguereau (1879)



A. lacerata – Karibik

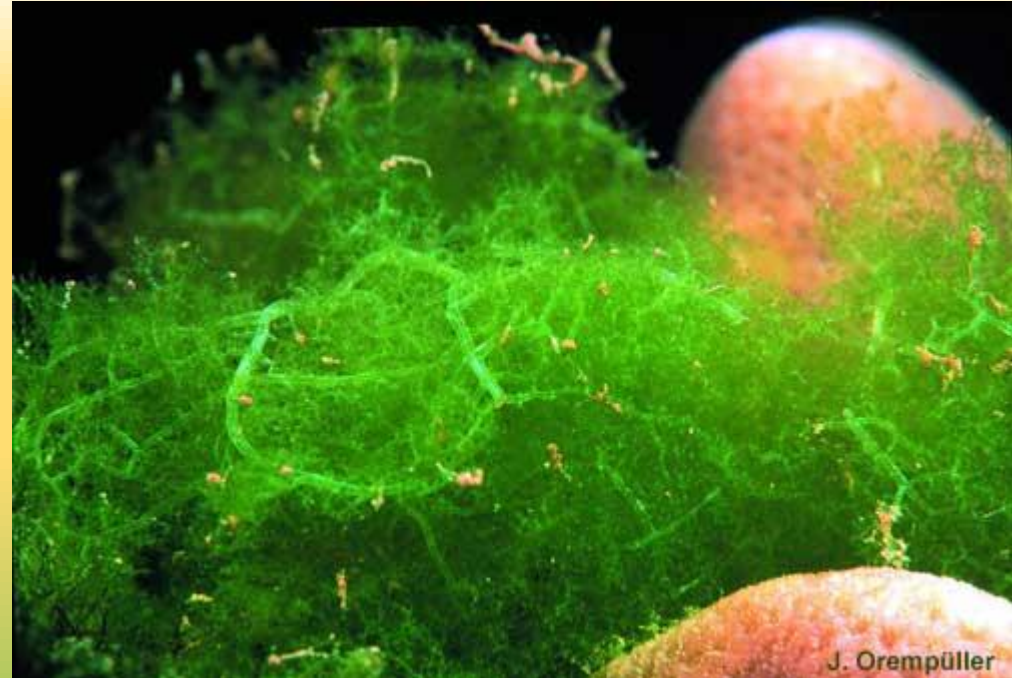
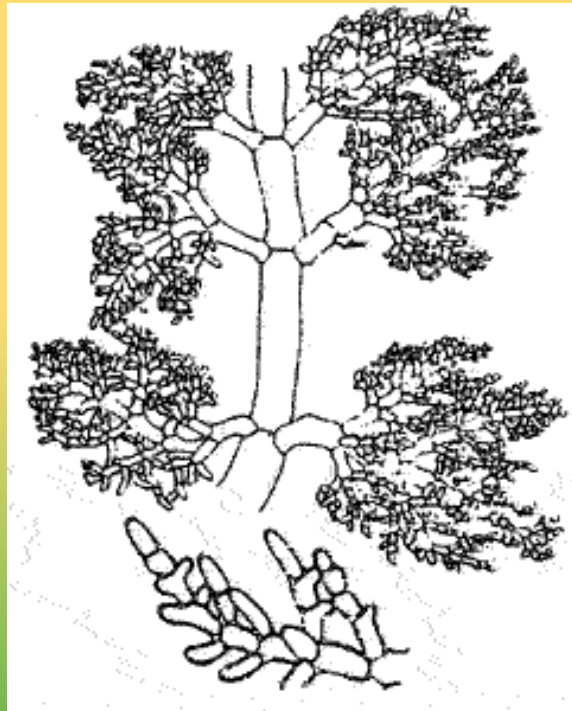
Cladophorales - *Siphonocladus* clade

Chamaedoris



Cladophorales - *Siphonocladus* clade

Boodlea



J. Orembüller



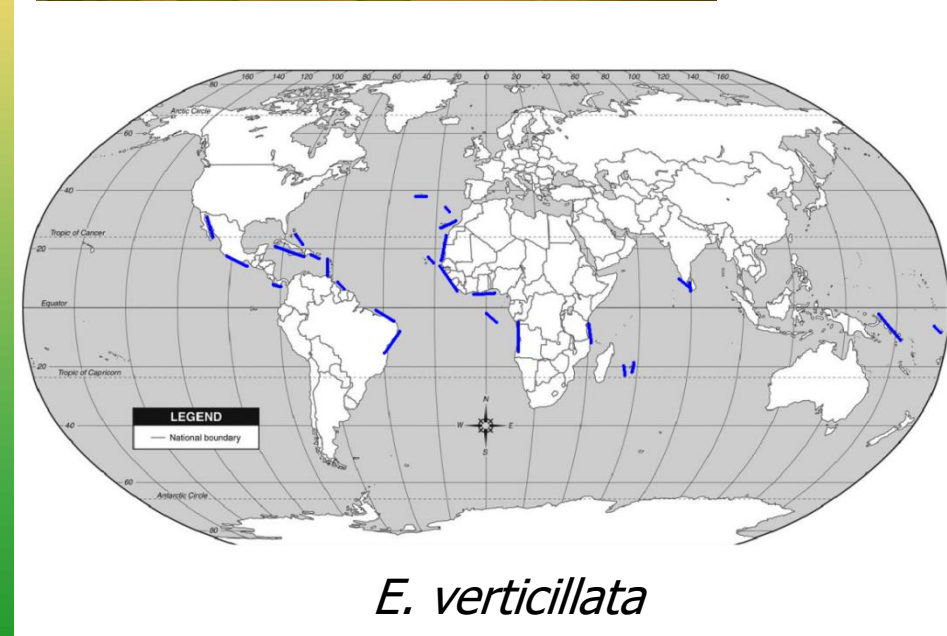
Cladophorales - *Siphonocladus* clade

Siphonocladus



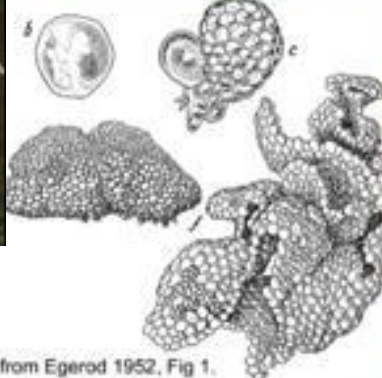
Cladophorales - *Siphonocladus* clade

Ernadesmis

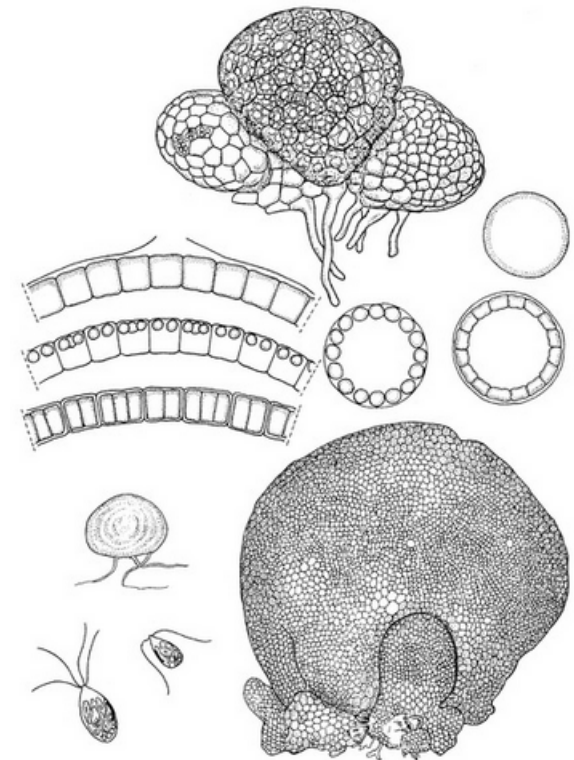


Cladophorales - *Siphonocladus* clade

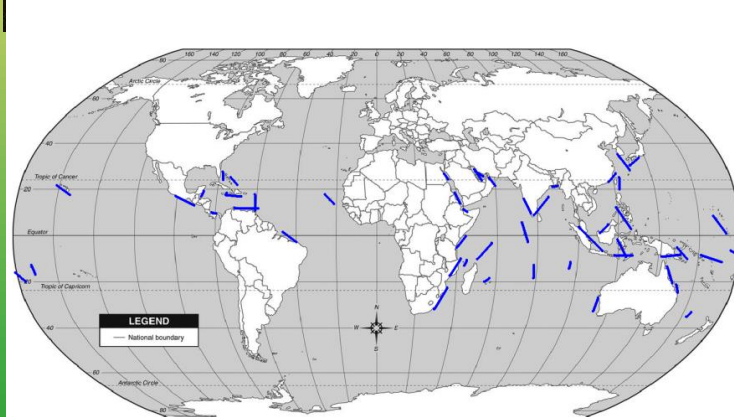
Dictyosphaeria



from Egerod 1952, Fig 1.



1, habit of a young specimen; 2, habit of a mature specimen; 3, cross-section of an undivided unicellular primary vesicle (diagrammatic); 4,5, formation of secondary vesicles inside the primary vesicle (cross-sections, diagrammatic); 6, the original wall of the primary vesicle has burst; 7, spherical protoplasmatic bodies are formed; 8, tertiary vesicles have been formed (6,7,8 diagrammatic cross-sections to show formation of tertiary vesicles); 9, habit of unicellular germling; 10, gamete with 2 flagella and an eyespot; 11, zoospore with 4 flagella and an eyespot.

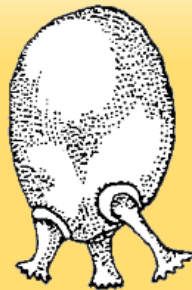
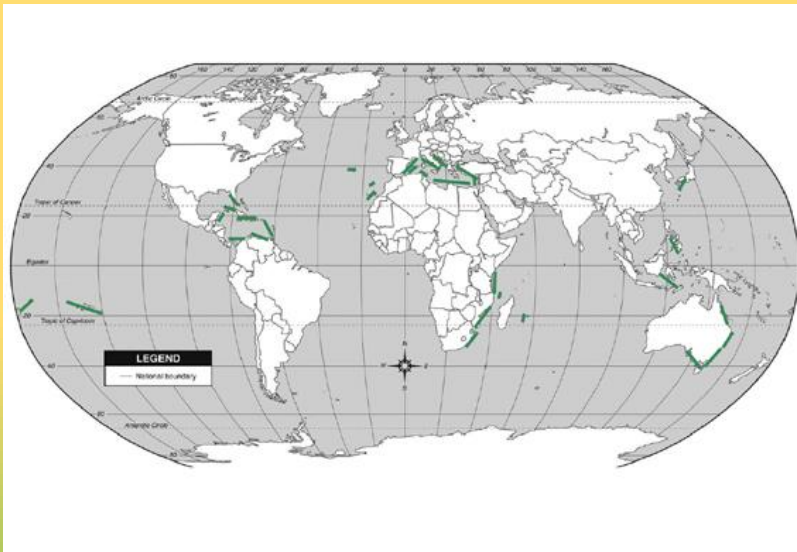


D. cavernosa



Cladophorales - *Siphonocladus* clade

Valonia



Valonia macrophysa

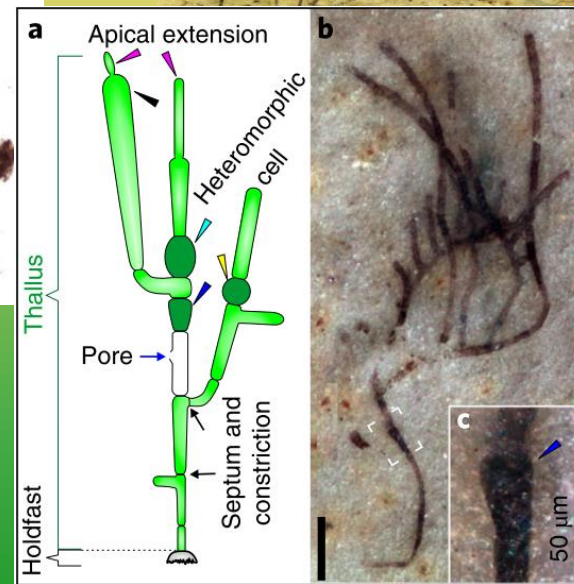
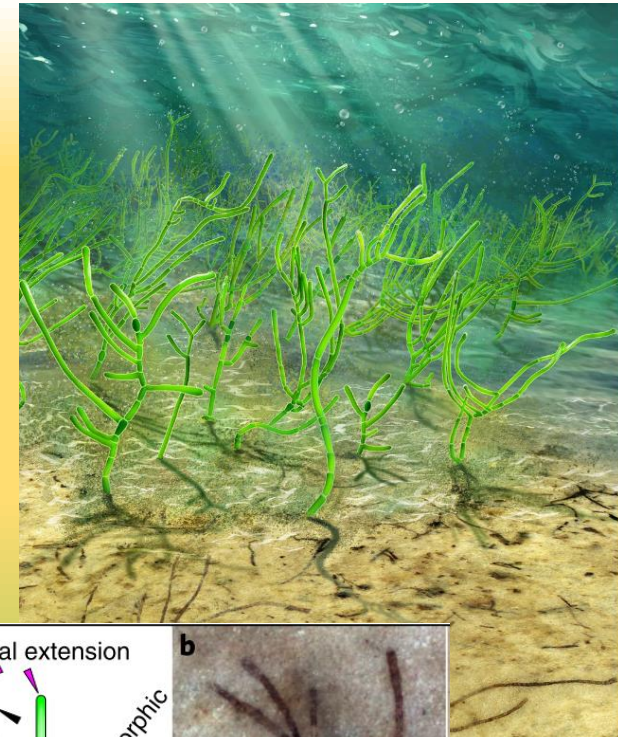
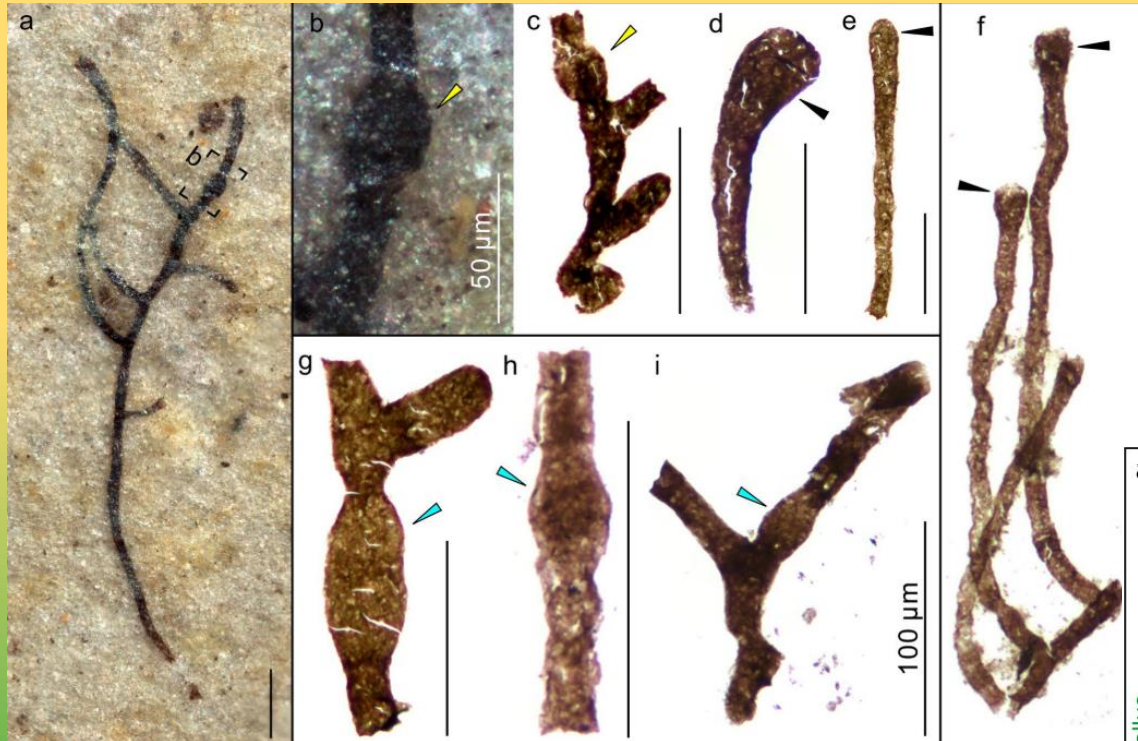


Valonia utricularis – Středozemní moře

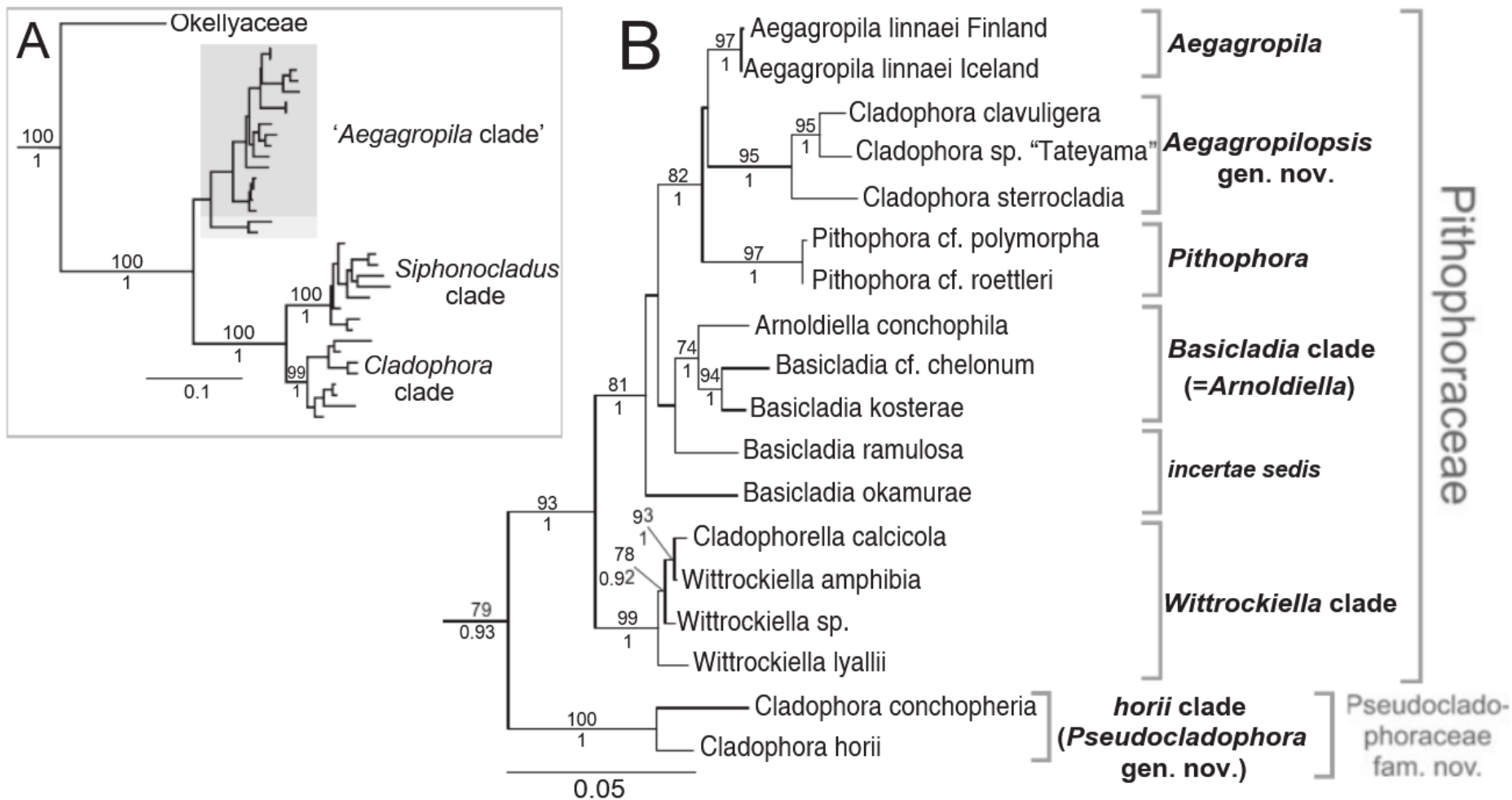


Cladophorales - *Siphonocladus* clade

Proterocladius antiquus



Cladophorales - *Aegagropila* clade

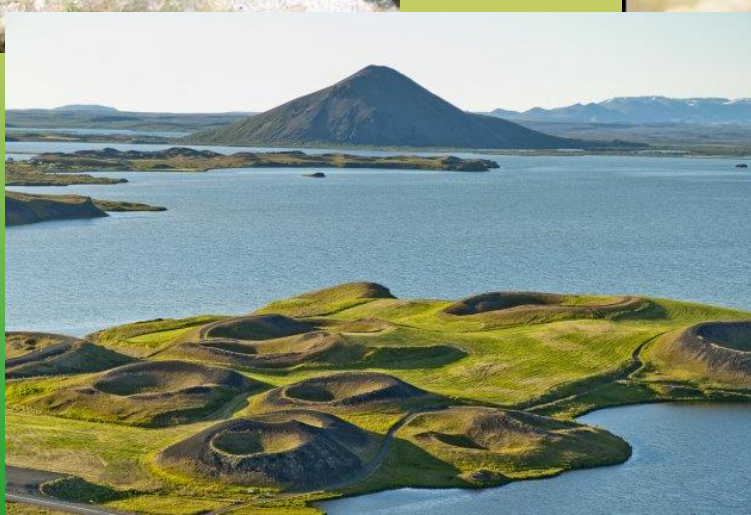


Cladophorales - *Aegagropila* clade

Aegagropila

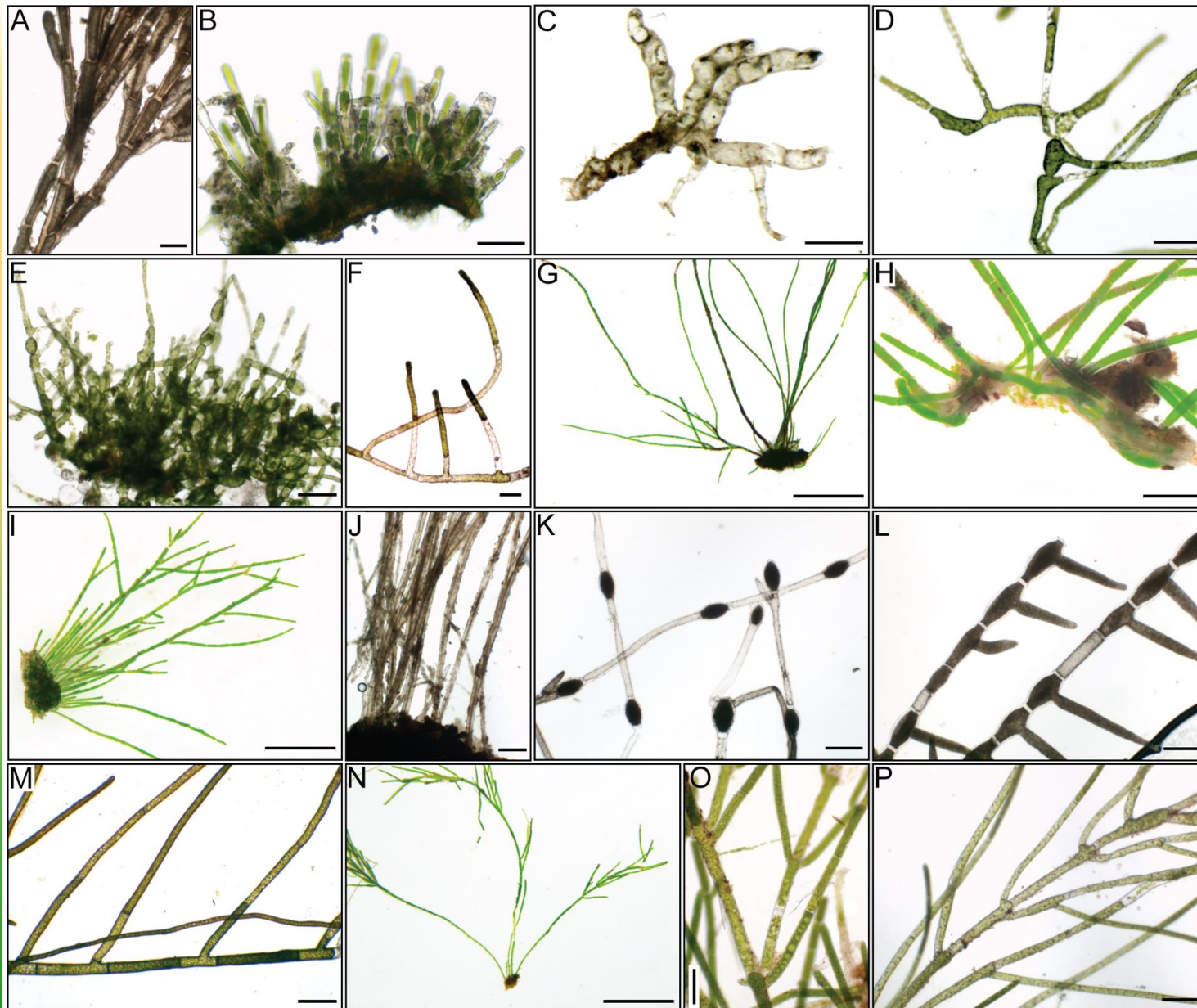


(c) Jeff Stout



Ljósmynd: Isamu Wakana

Cladophorales - *Aegagropila* clade



Boedekker
et al. (2012)

Cladophorales

Aegagropila clade

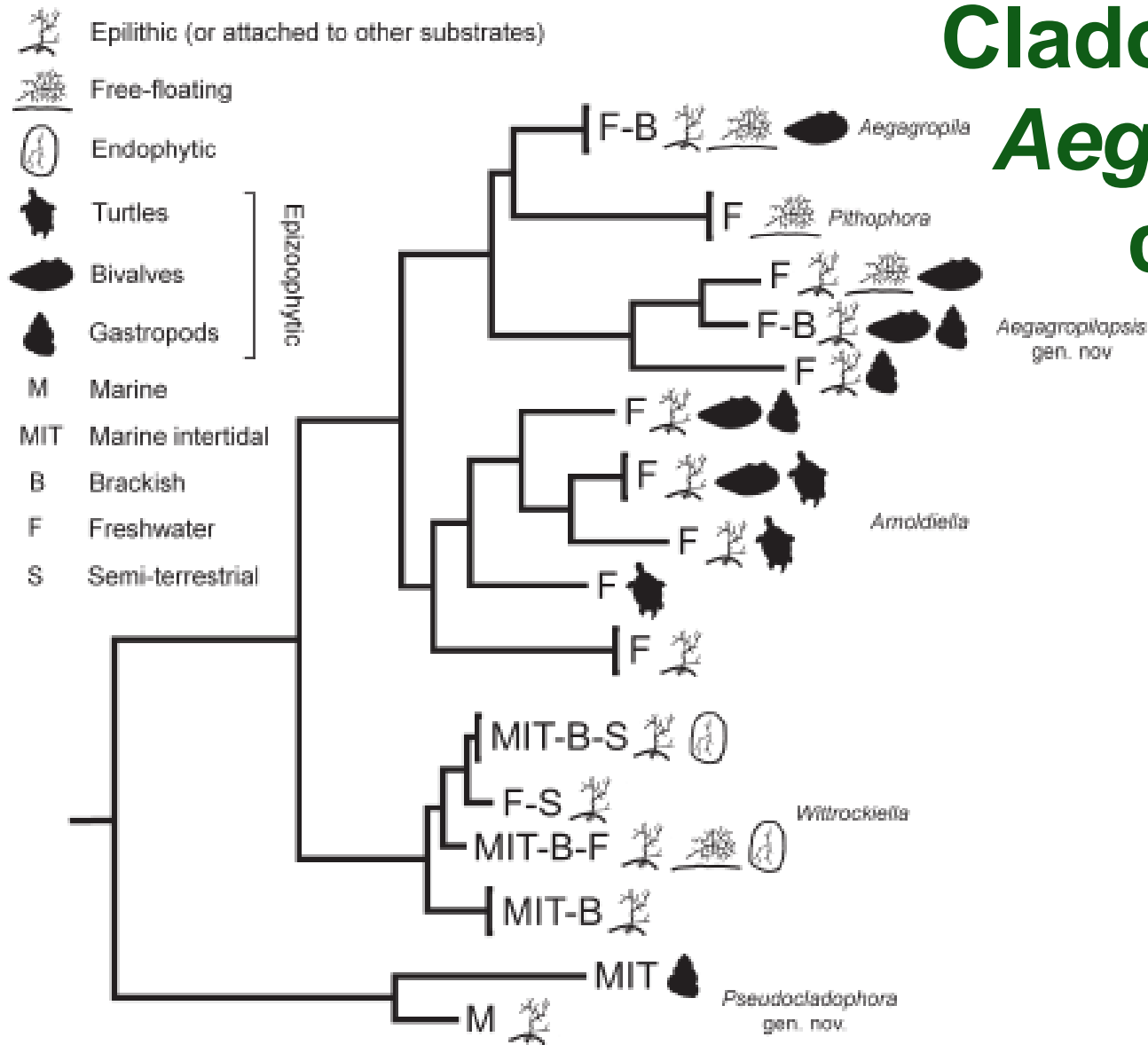
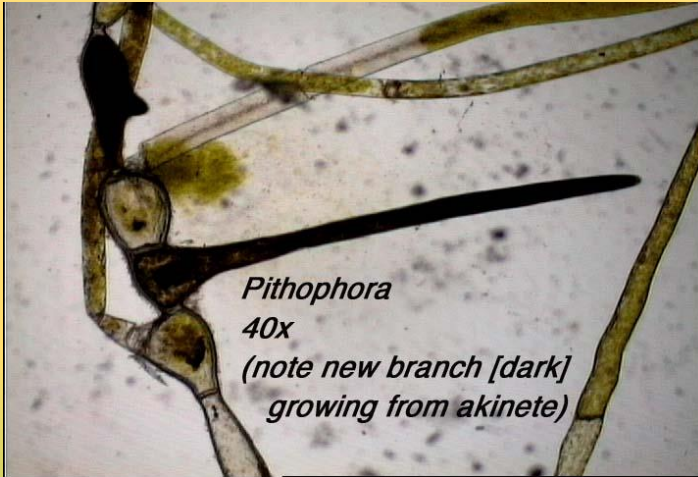


Figure 7. Phylogenetic tree of the *Aegagropila*-lineage (same as Fig. 4B), with letters indicating environment types in which the taxa occur, and stylised symbols indicating known host animals of epizoophytic taxa and growth forms.

Boedekker
et al. (2012)

Cladophorales - *Aegagropila* clade

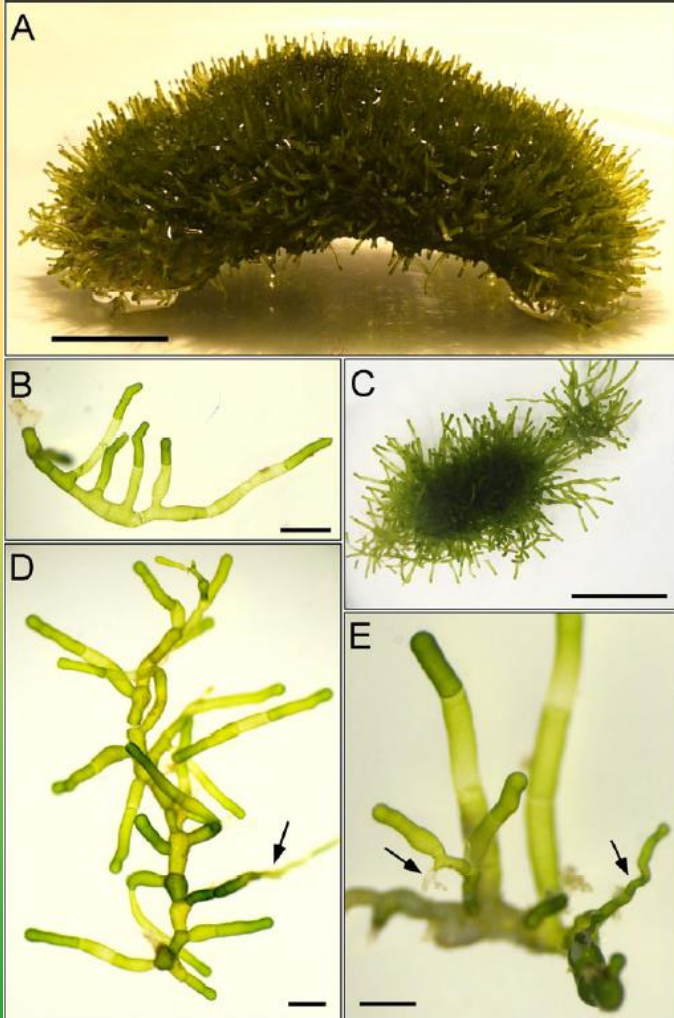
Pithophora



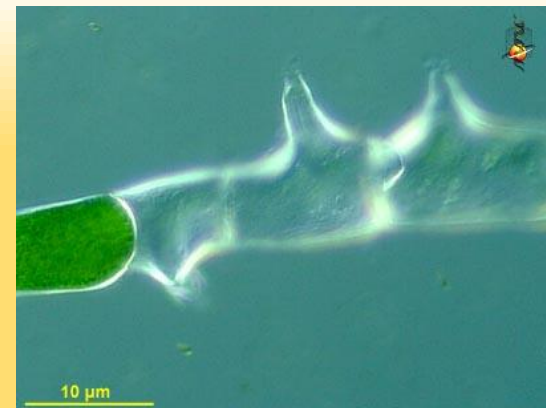
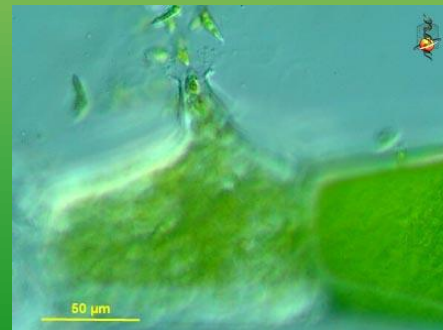
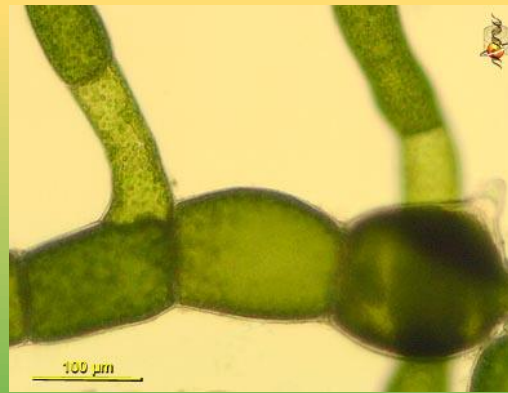
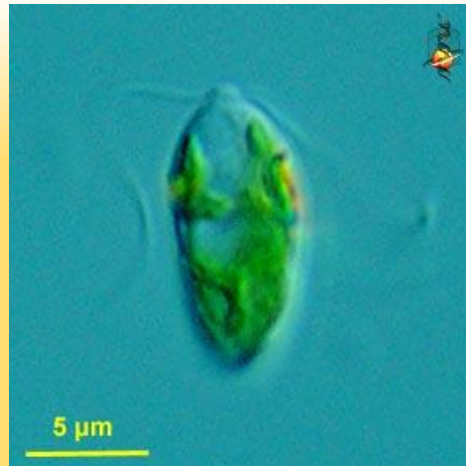
Florida – freshwater metaphyton

Cladophorales - *Aegagropila* clade

Wittrockiella



Boedeker et al. (2017)



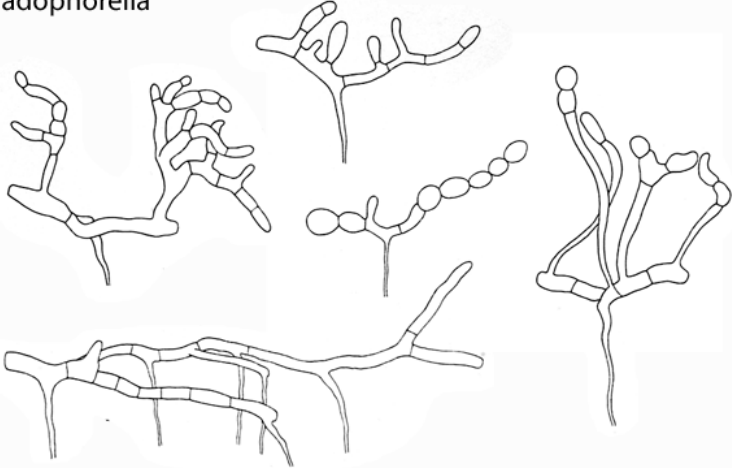
Doubtful Sound, NZ



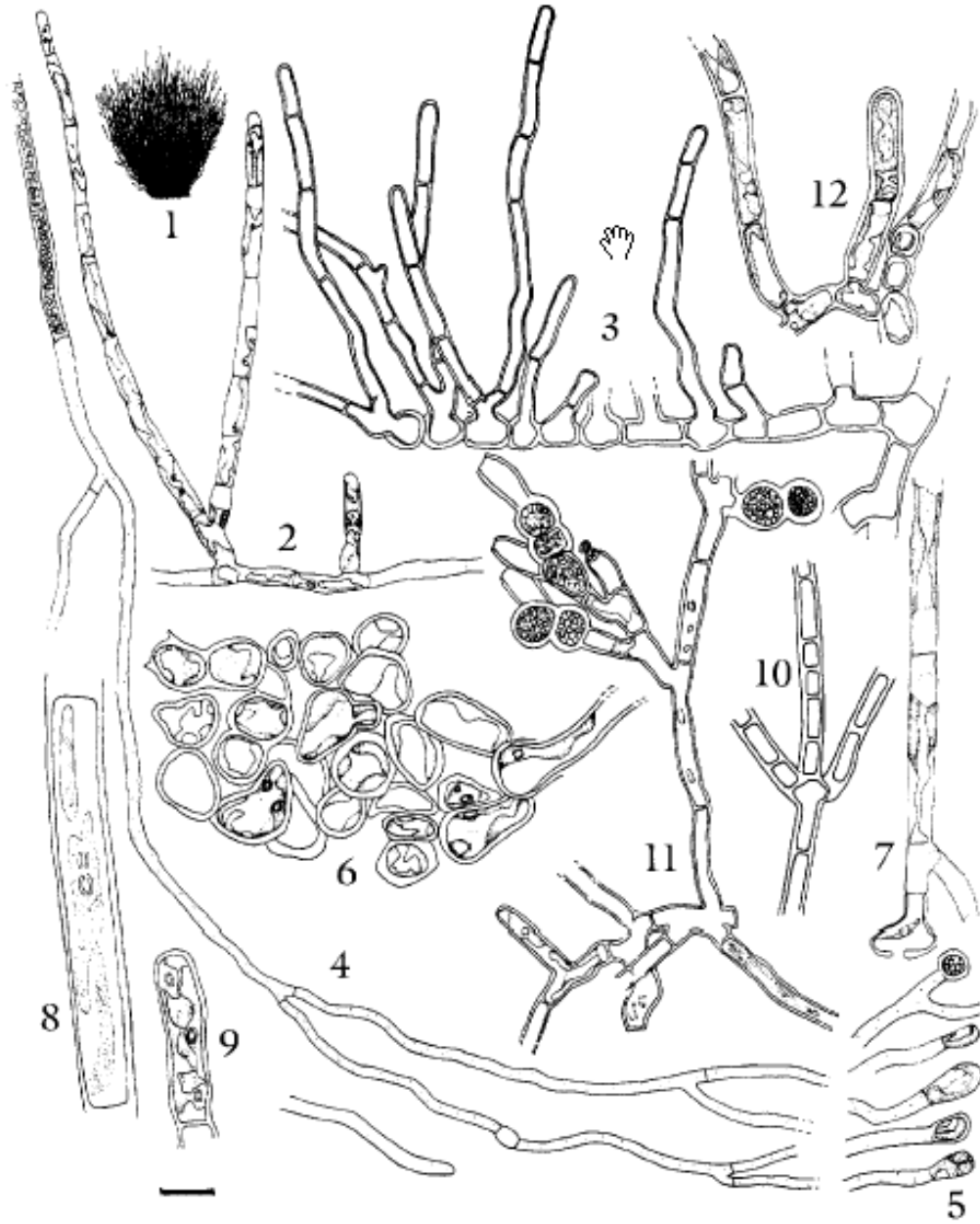
Cladophorales - *Aegagropila* clade

Cladophorella

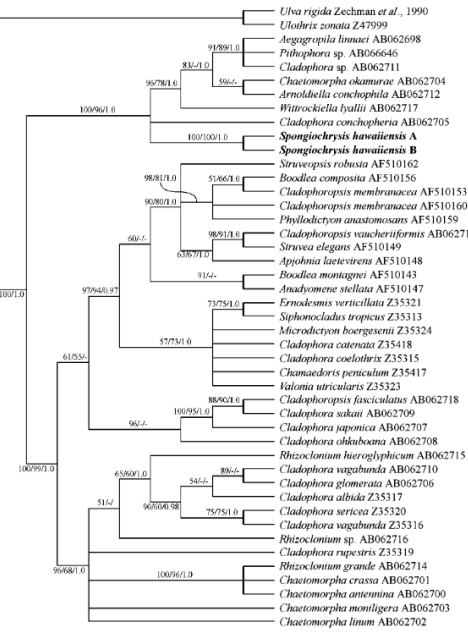
Cladophorella



After Cribb (1965b)



Spongiochrysis hawaiiensis



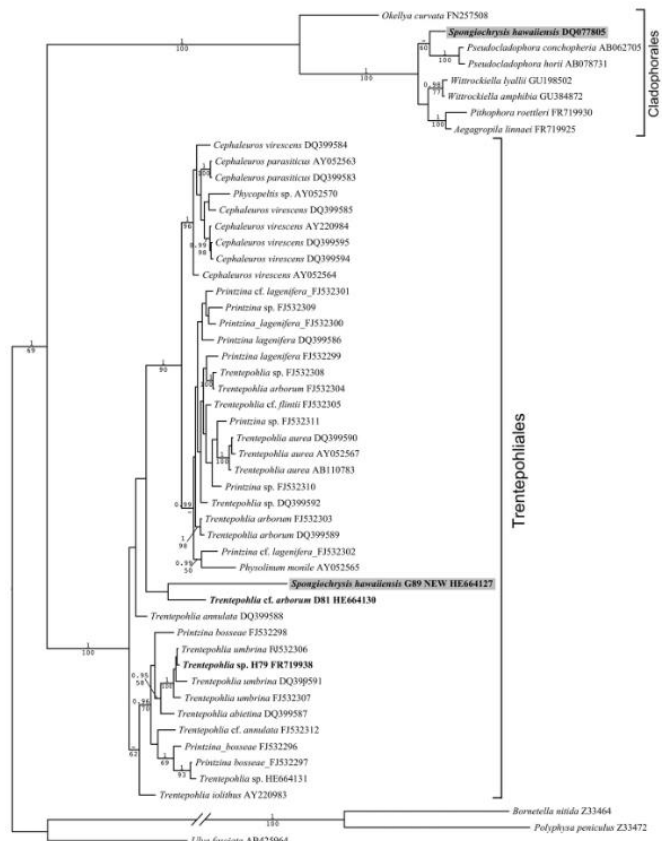
Rindi et al. (2006)

► Cladophorales

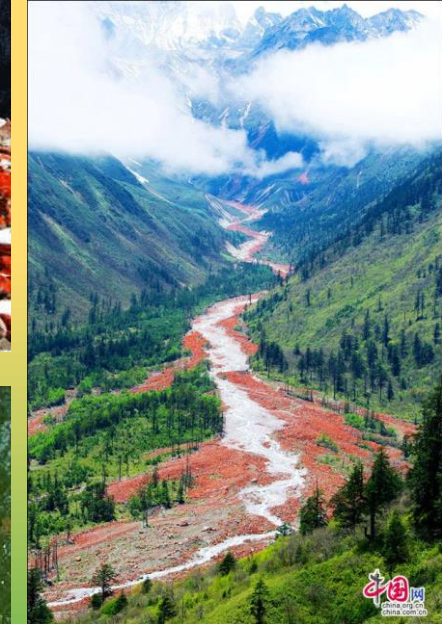


Johnston et al. (2018)
► Cladophorales !!

Spongiochrysis is in Trentepohliales



Ulvophyceae - Trentepohliales



Základní charakteristika

Terestrické

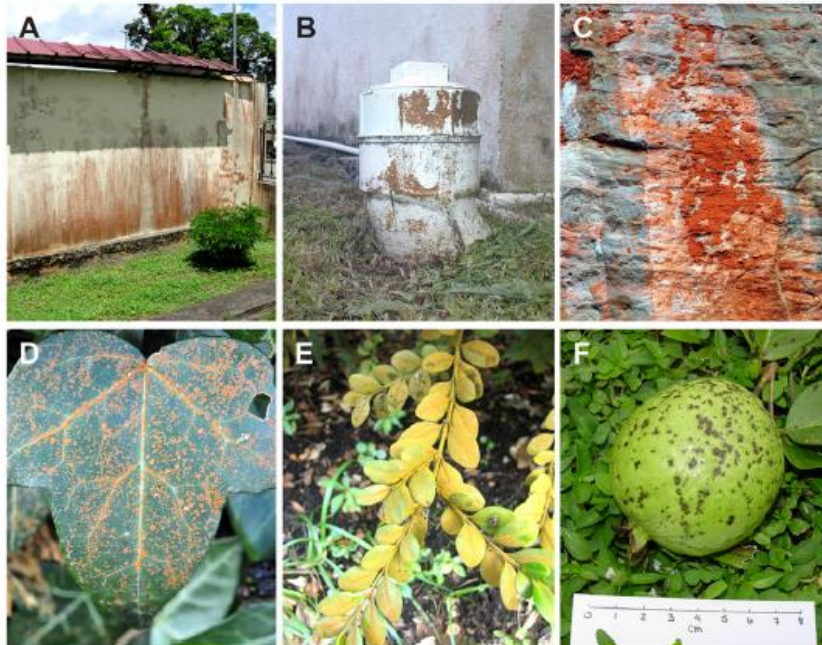
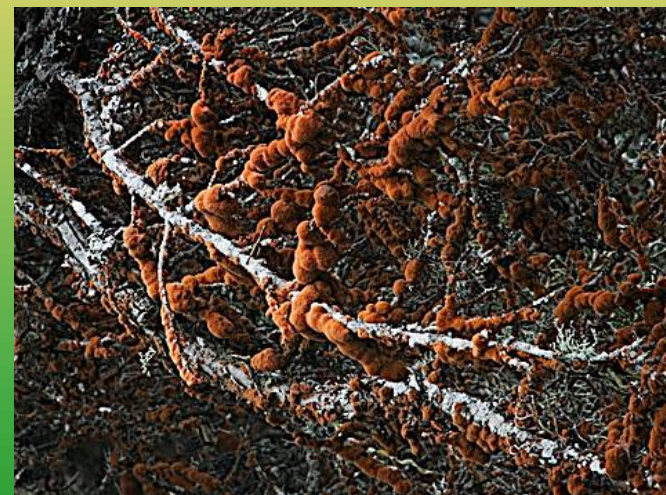


Fig. 2. Genera of the Trentepohliales are widely distributed and grow on living and nonliving substrates. **A.**, Sinnamary, French Guiana: Species of *Trentepohlia* stain numerous porous surfaces reddish orange. **B.**, American Samoa: *Trentepohlia* even lives on nonporous plastics. **C.**, Devil's Punchbowl, Oregon: *Trentepohlia flava* growing on the inner rim of a rocky bowl carved by the sea. **D.**, Moyullen, Ireland: *Phycopeltis* is a common epiphyte, often with beautifully symmetrical thalli. **E.**, Heavy yellowish epiphytic growth of *Printzina lagenifera*. **F.**, American Samoa: *Cephaleuros virescens* is one of several species that cause plant damage, like this algal spot of guava (*Psidium guajava*) fruit.

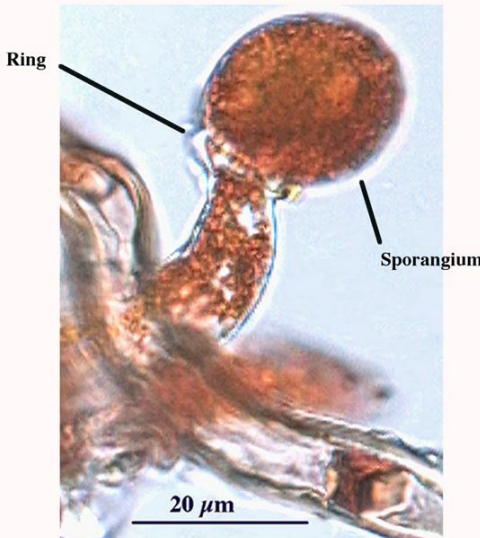
Brooks et al. (2015)

Sekundární karotenoidy



Základní charakteristika

Typická sporangia



López-Bautista et al. (2002)

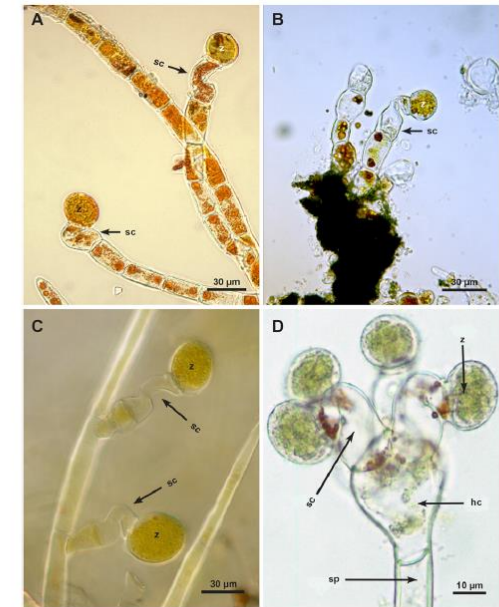
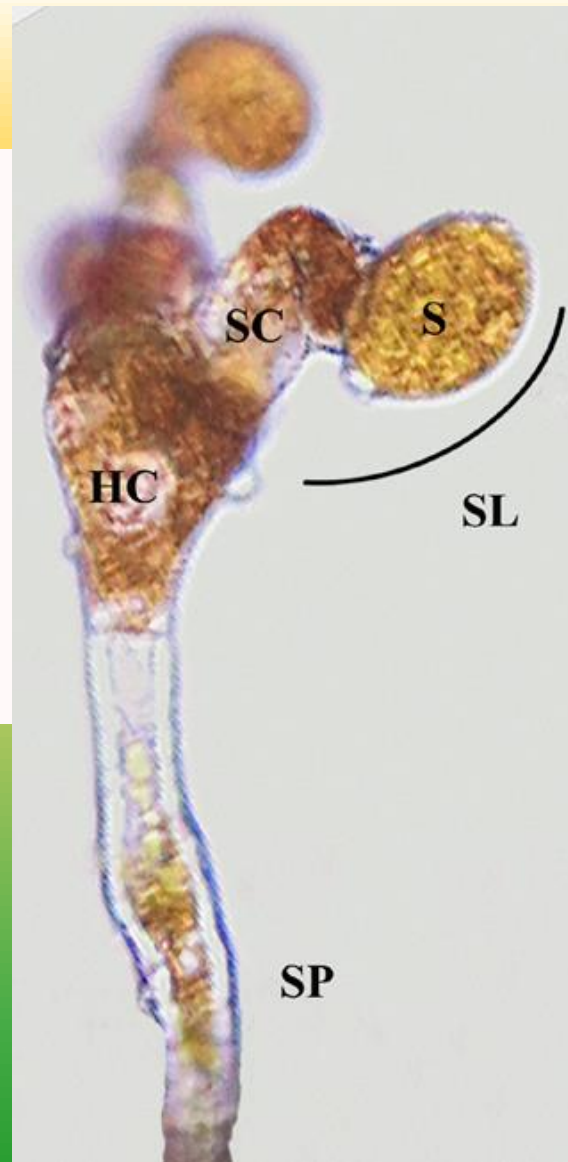


Fig. 3. The sporangiate-lateral is unique to the Trentepohliales. It consists of a zoosporangium (z) borne at the end of a crooked "sufflitory" cell (sc). When moisture is present the cell straightens, holding the sporangium away from the sporangiophore (sp) and head cell (hc) and promoting windborne dispersal. A, *Trentepohlia* sp.; B, *Printzia* sp.; C, *Cephaleuros minimus*; D, *Virescens*.

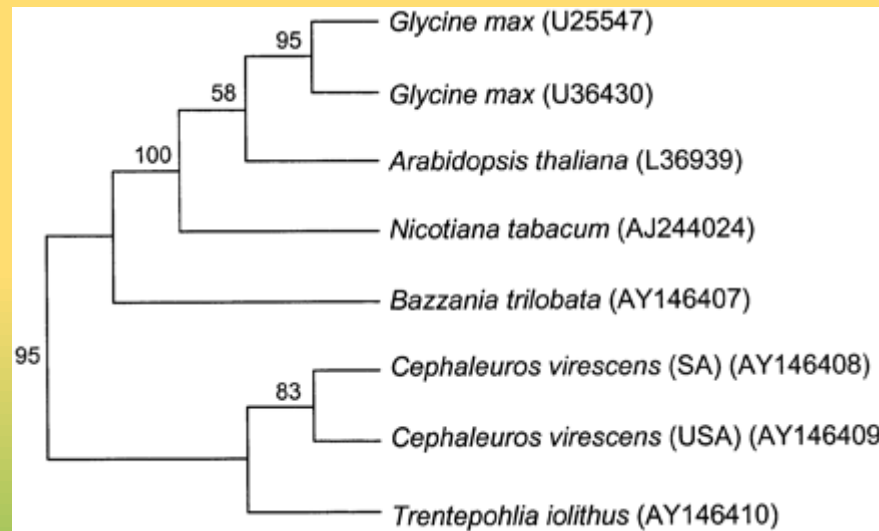
Izomorní i heteromorfni
rodozměna

Základní charakteristika



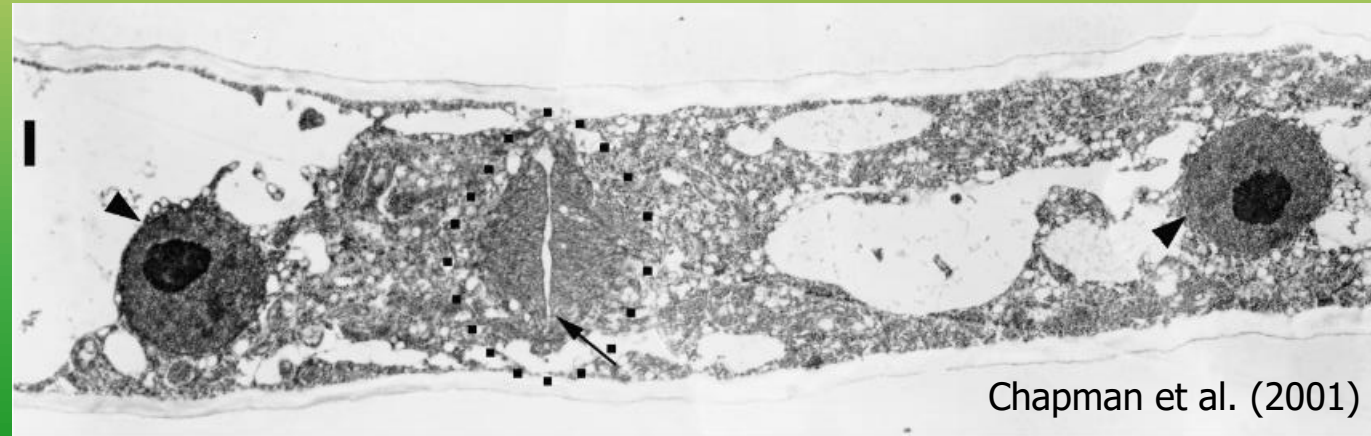
Plasmodesmy

Bičíkatá stadia nemají stigma a mají strukturu připomínající MLS, nemají pyrenoidy



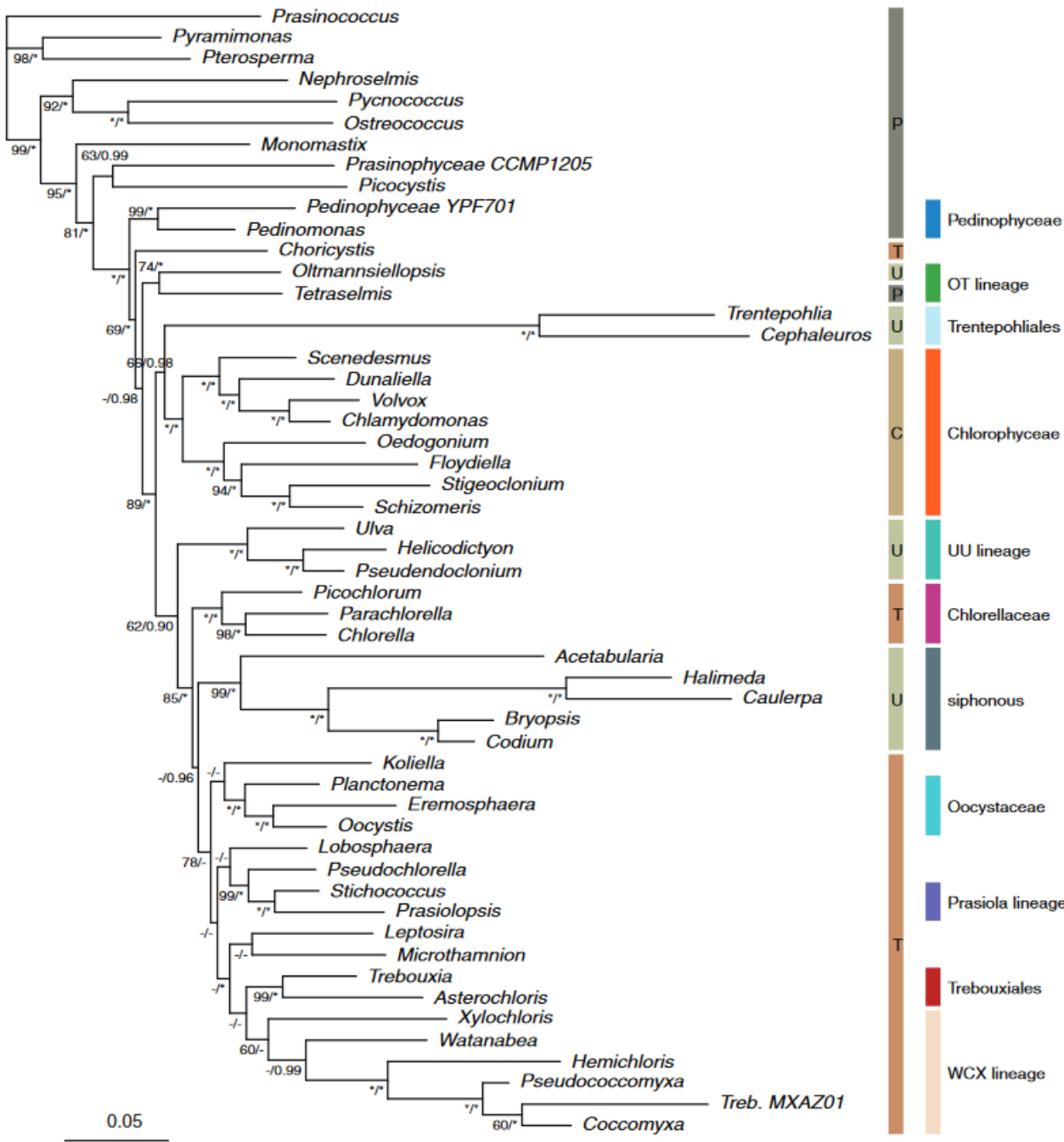
Fragmoplast

López-Bautista et al.
(2003)



Chapman et al. (2001)

Evoluce



Fučíková et al. (2014)

Evolute

Tradiční rody:

Trentepohlia
Phycopeltis
Cephaleuros
Stomatochroon
Printzina

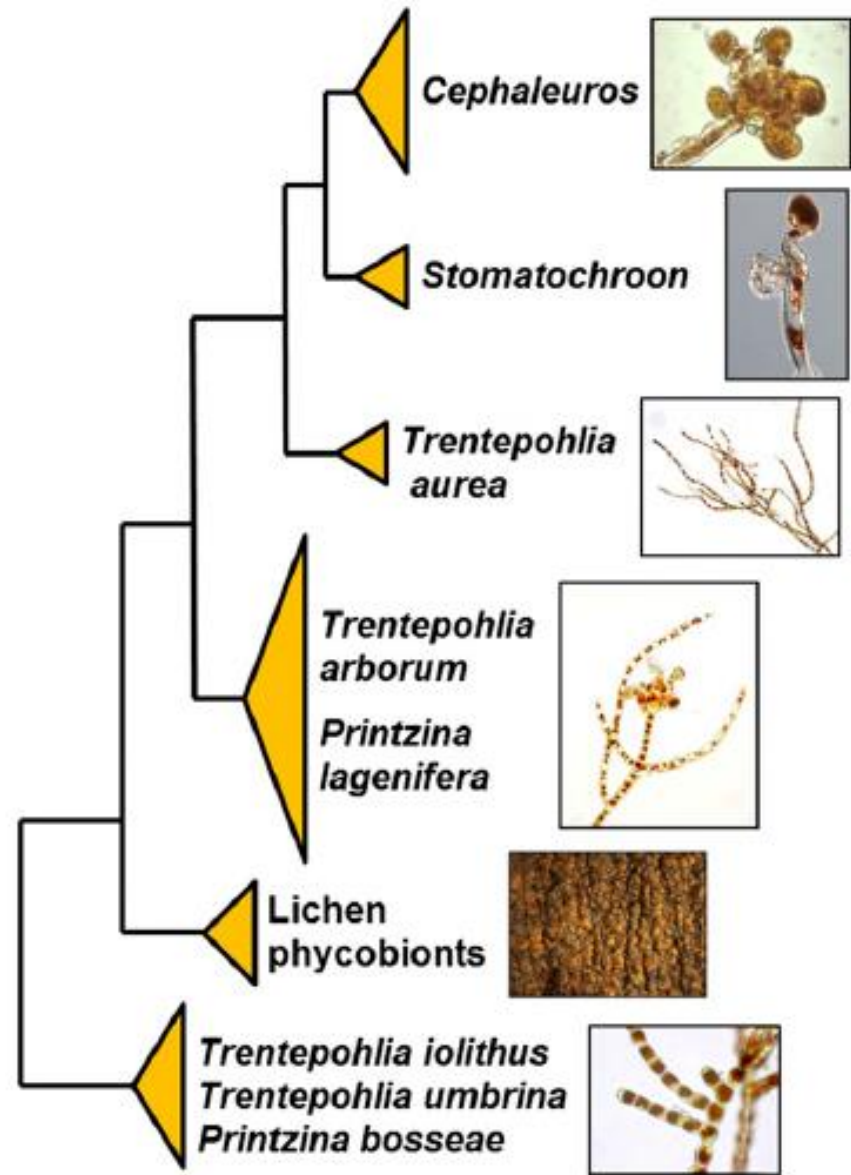
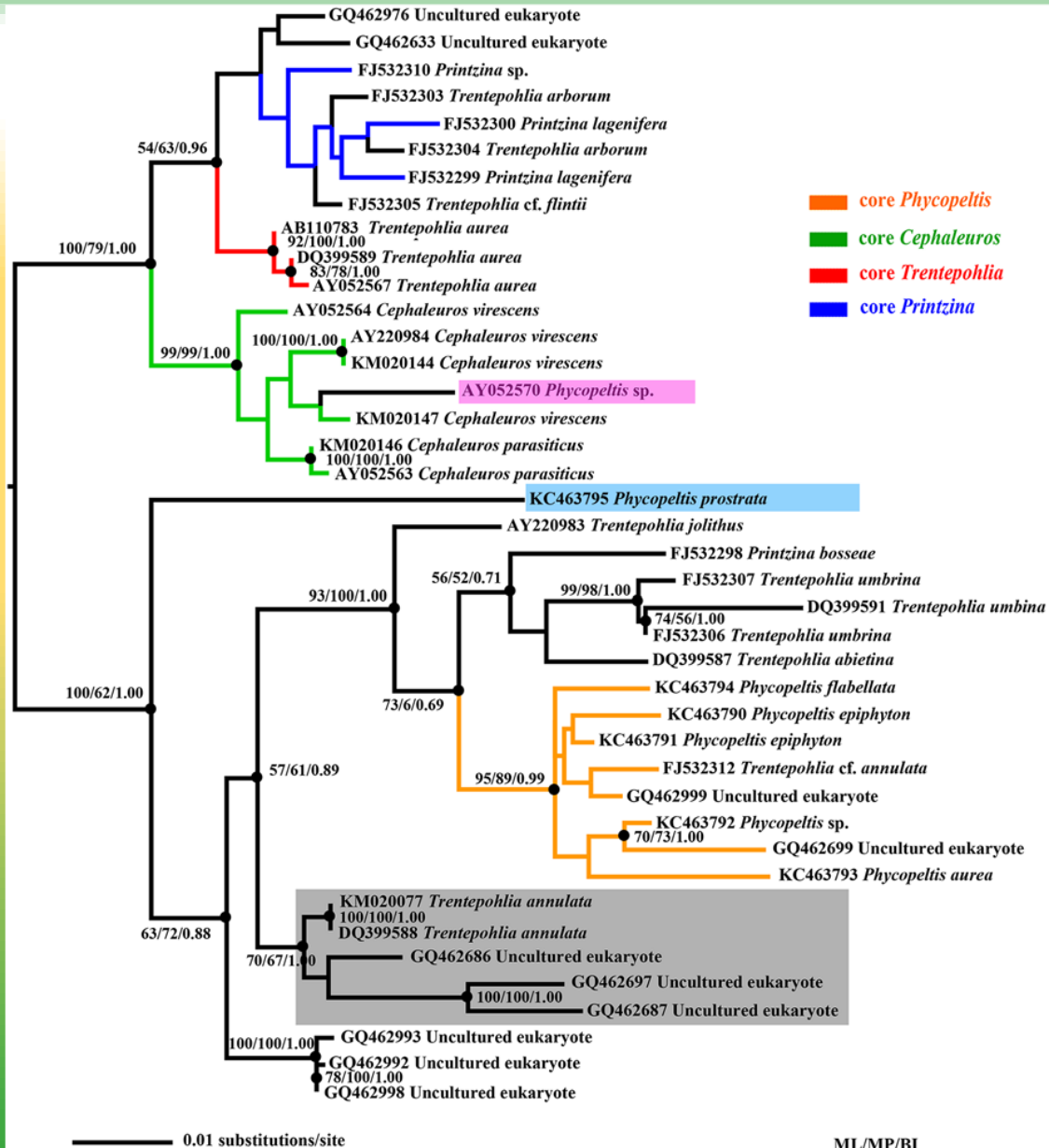


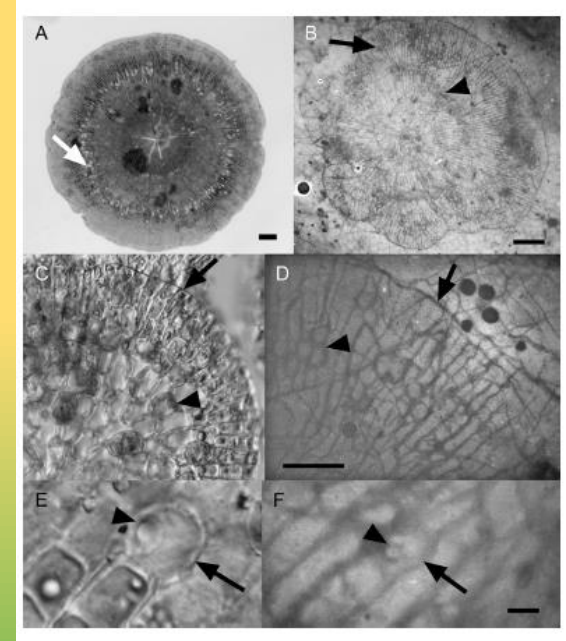
Fig. 4. Summary of phylogenetic relationships within the Trentepohliales based on molecular data from López-Bautista et al. 2006, Nelsen et al. 2011, Rindi et al. 2009, and Zhu et al. 2014. Stomatochroon photo courtesy of G.-X. Liu.

Evolute



SSU rDNA

Zhu et al. (2015)



Novis et al. (2015)

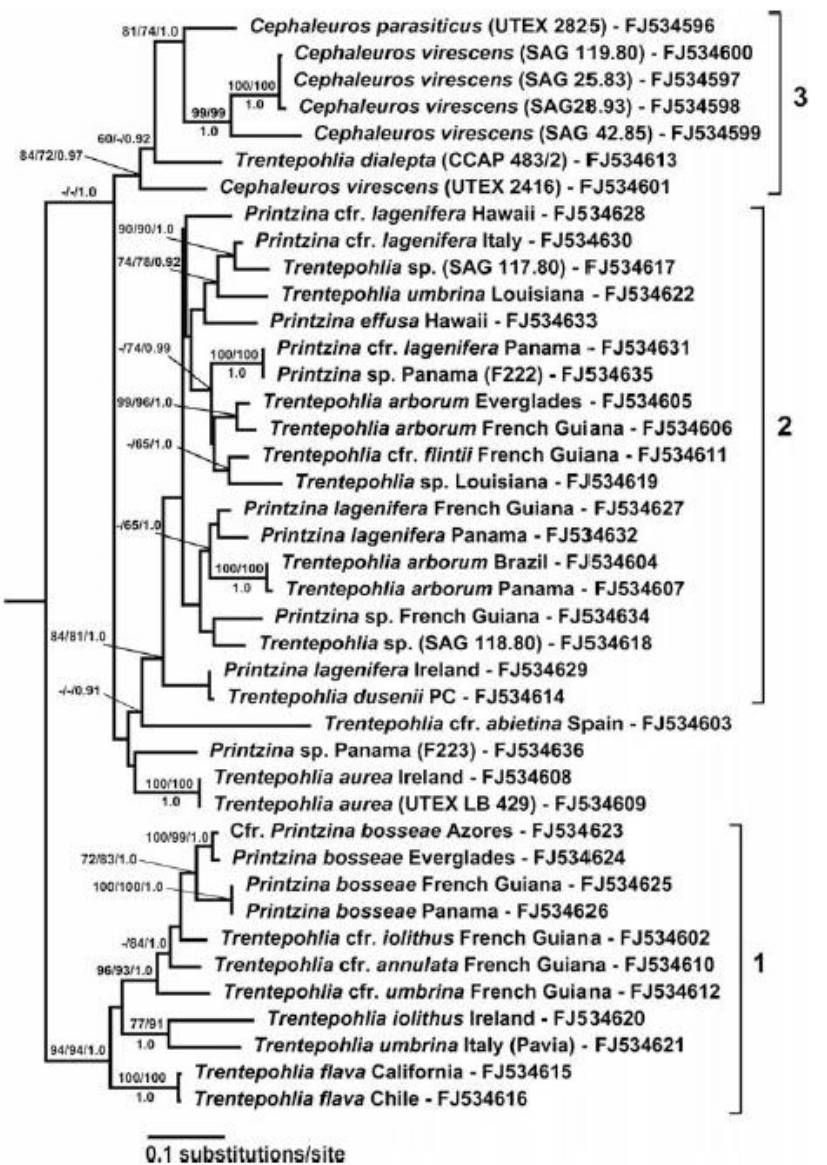


Fig. 2. Phylogenetic tree inferred from Maximum Likelihood analysis of the *rbcL* gene in *Trentepohlia*, *Printzina* and related taxa, with bootstrap support (BP) and Bayesian posterior probabilities (PP) indicated at the nodes. From left to right (or from top to bottom, above and below branches), support values at nodes correspond to Maximum Parsimony BP, Maximum Likelihood BP and Bayesian PP. BP values lower than 60% and PP lower than 0.85 are not reported. The tree was rooted using outgroup sequences of Dasycladales and Bryopsidales (not shown) specified in Section 2.

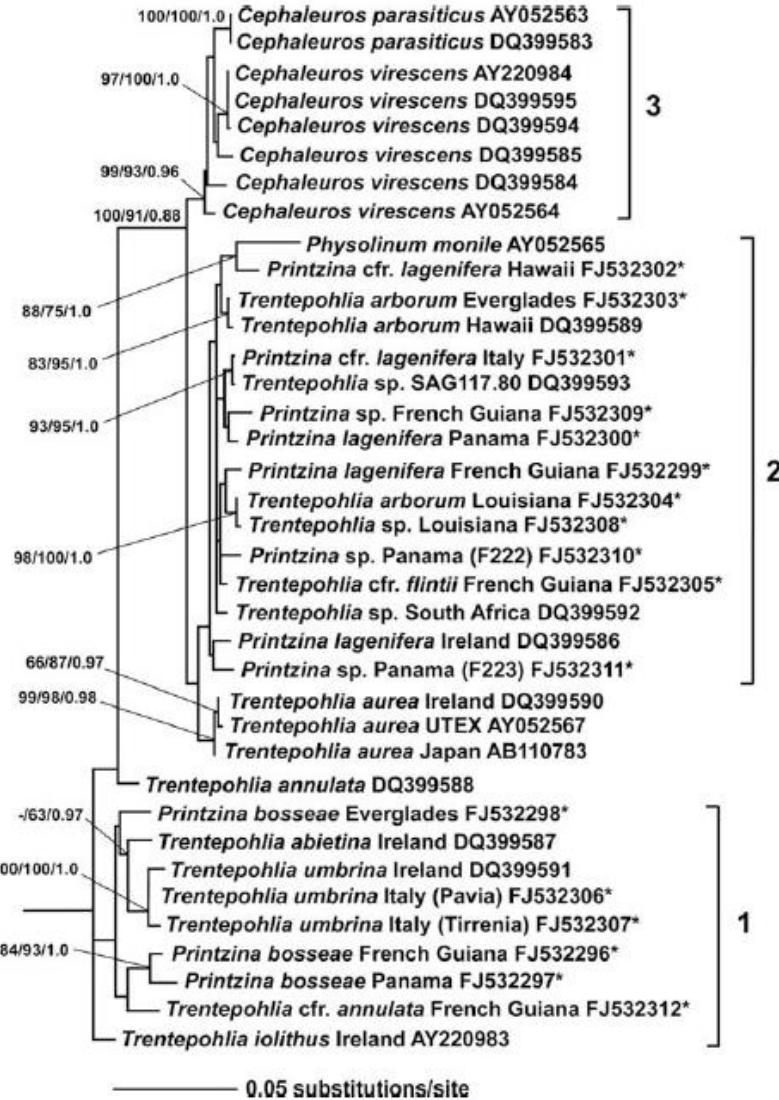


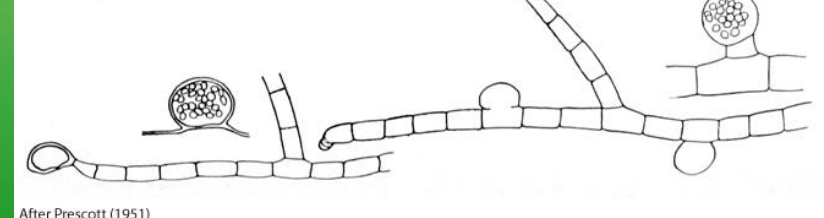
Fig. 3. Phylogenetic tree inferred from Maximum Likelihood analysis of the 18S rRNA gene in *Trentepohlia*, *Printzina* and related taxa, with bootstrap support (BP) and Bayesian posterior probabilities (PP) indicated at the nodes. From left to right support values at nodes correspond to Maximum Parsimony BP, Maximum Likelihood BP and Bayesian PP. BP values lower than 60% and PP lower than 0.85 are not reported. The tree was rooted using outgroup sequences of Cladophorales and Dasycladales (not shown) specified in Section 2. New sequences produced in the present study are marked with an asterisk.

Trentepohliales – přehled rodů

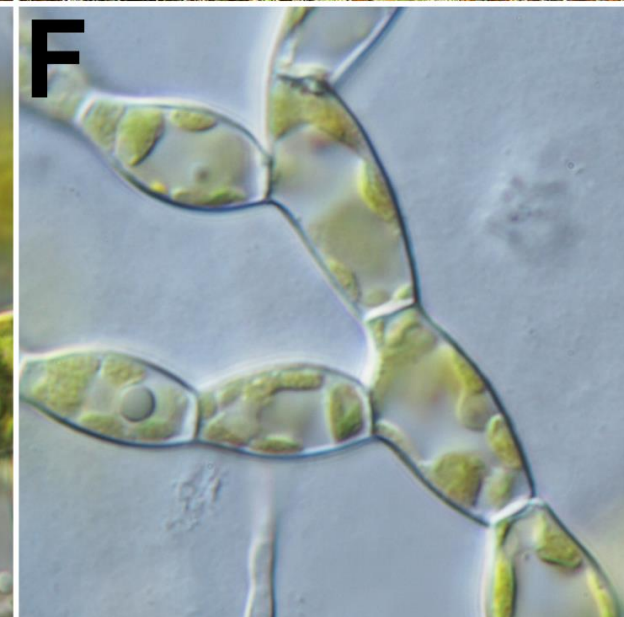
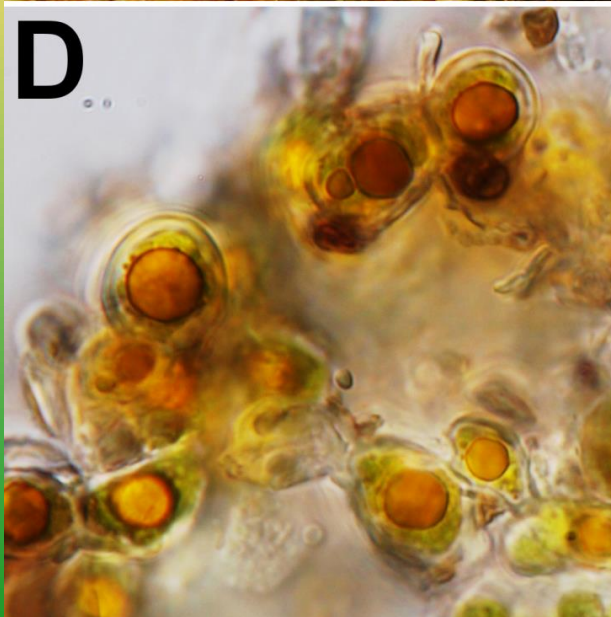
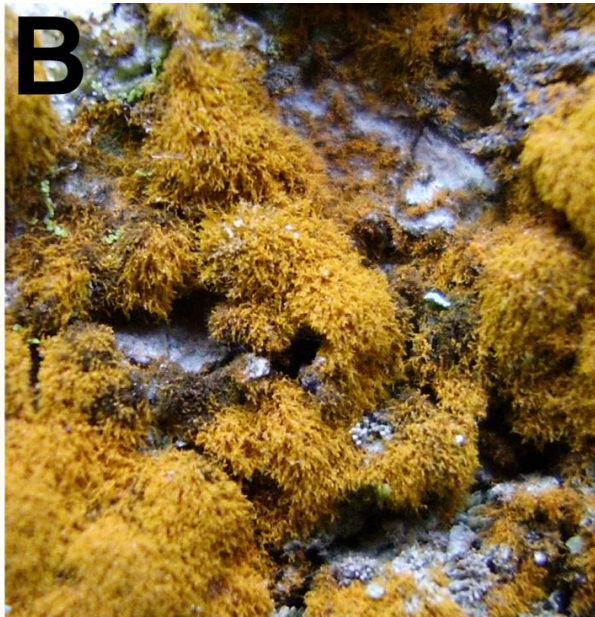
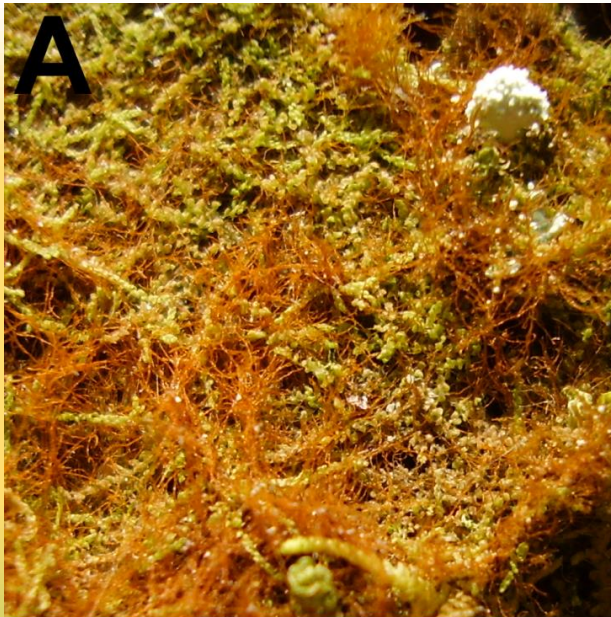
Trentepohlia



Trentepohlia

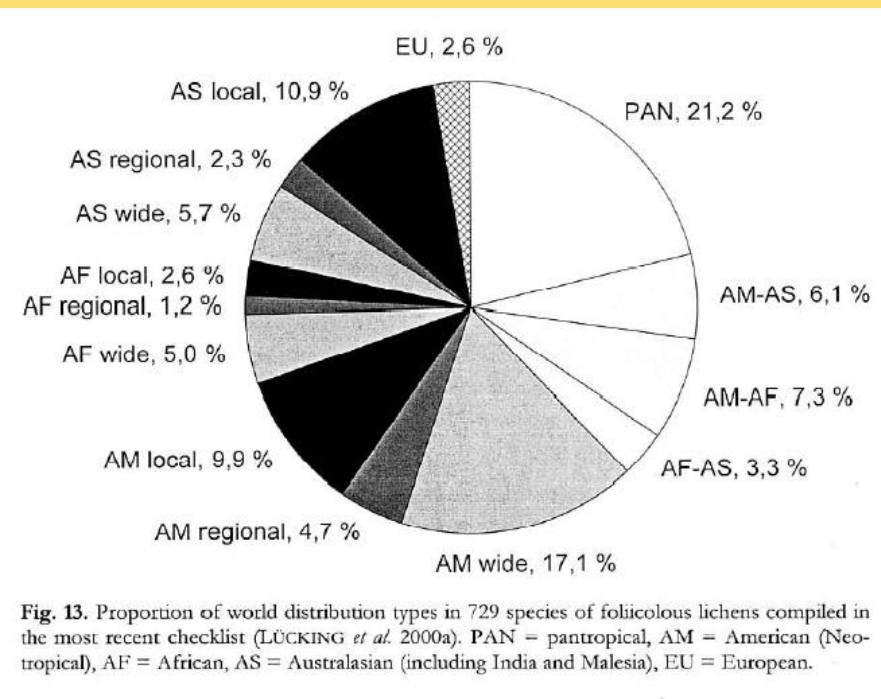


Trentepohlia



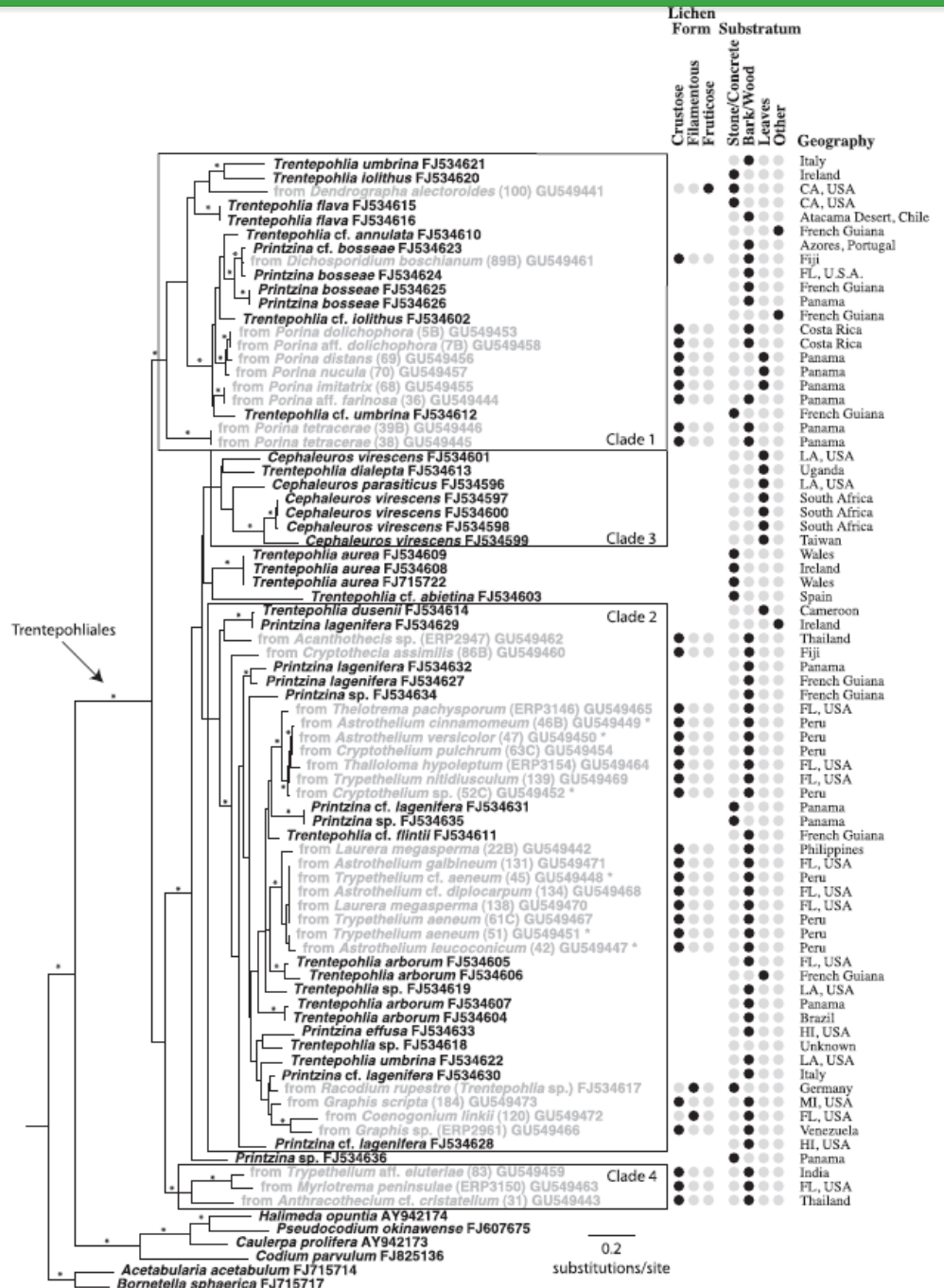
Trentepohliales – přehled rodů

Trentepohlia – folikolní lišejníky



Trentepohliales přehled rodů

Trentepohlia



Nelsen et al. (2011)

FIG. 1. Maximum-likelihood (ML) phylogeny of Trentepohliales algae based on *rbdL* sequence data. *Acetabularia acetabulum* and *Bornetella sphaerica* were used to root the tree. Black asterisks above or below branches indicate strong support (ML bootstrap ≥70 and BI posterior probability ≥0.95) for that clade. Non-lichenized holotypes are listed in black, while lichenized holotypes are in gray. Gray asterisks following the species name indicate that the species is lichenized.

Trentepohliales – přehled rodů

Trentepohlia

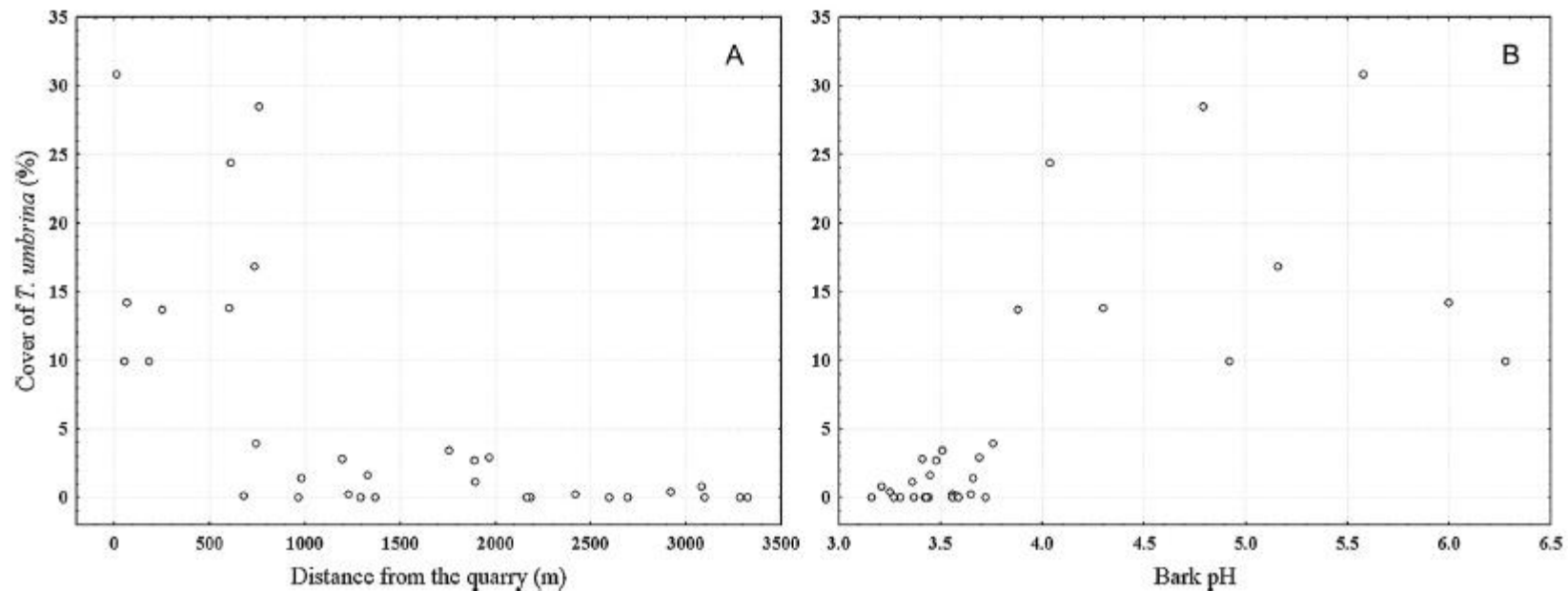
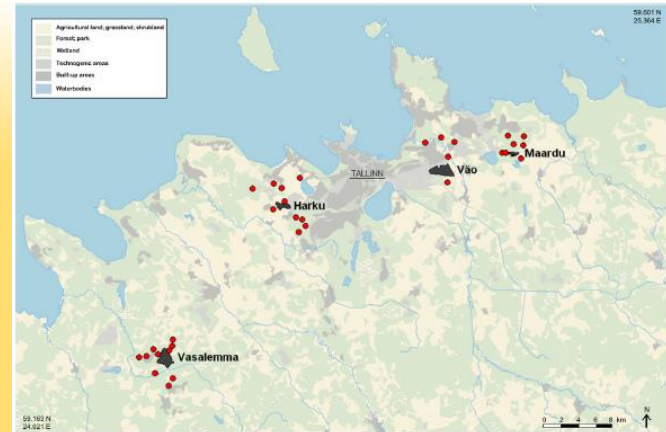
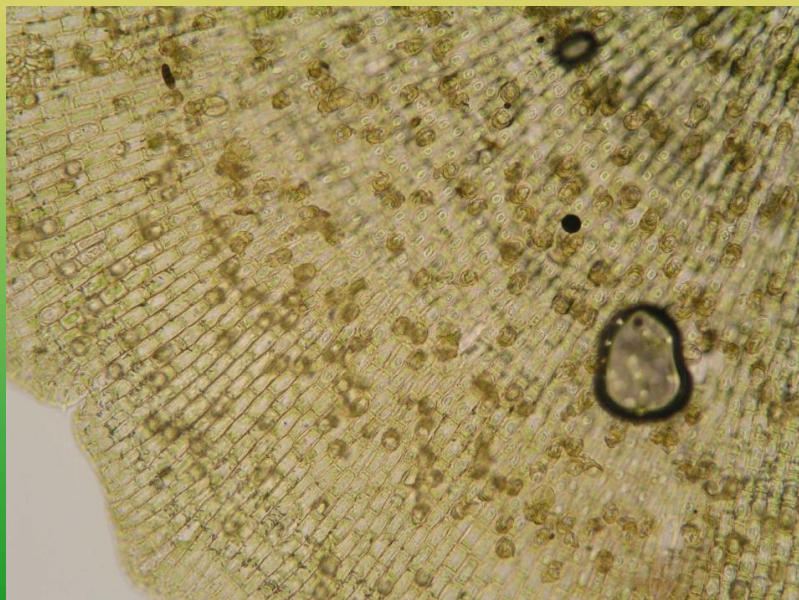
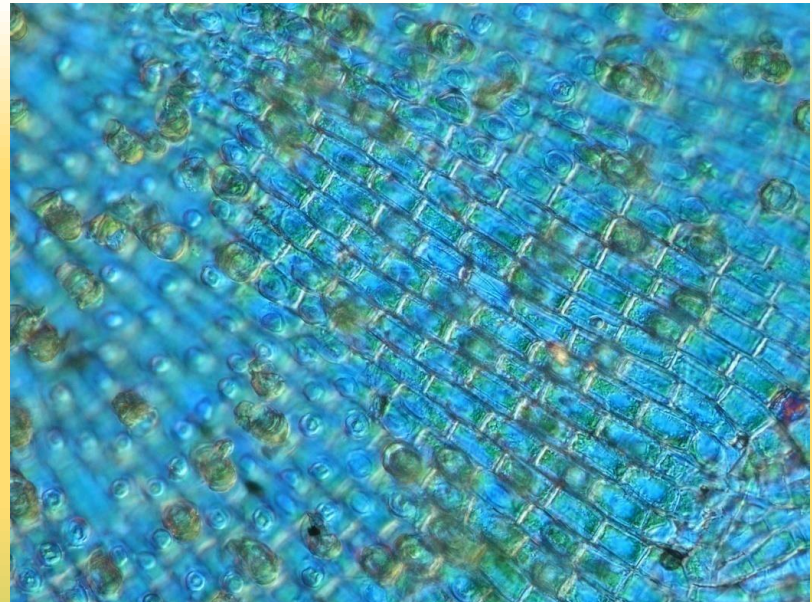


Fig. 2. Correlation of *Trentepohlia umbrina* cover on pine trunks with (A) distance from the quarry ($R_s = -0.74$; $n = 32$; $p < 0.00001$), and (B) bark pH ($R_s = 0.72$; $n = 32$; $p < 0.00001$).

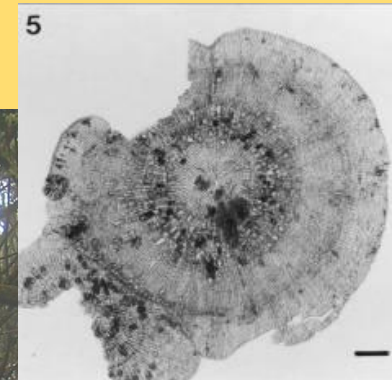
Trentepohliales – přehled rodů

Phycopeltis

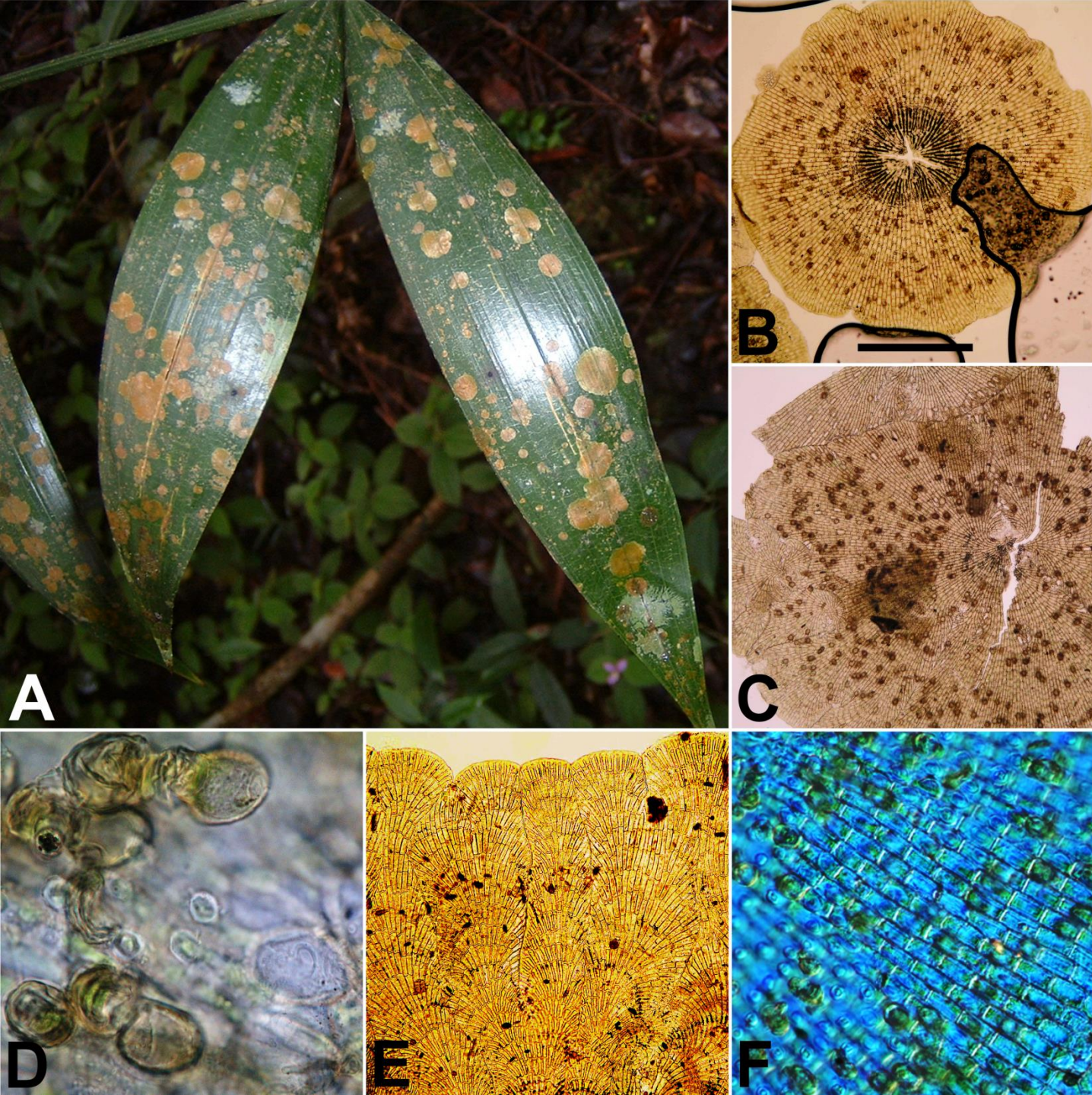


Trentepohliales – přehled rodů

Phycopeltis

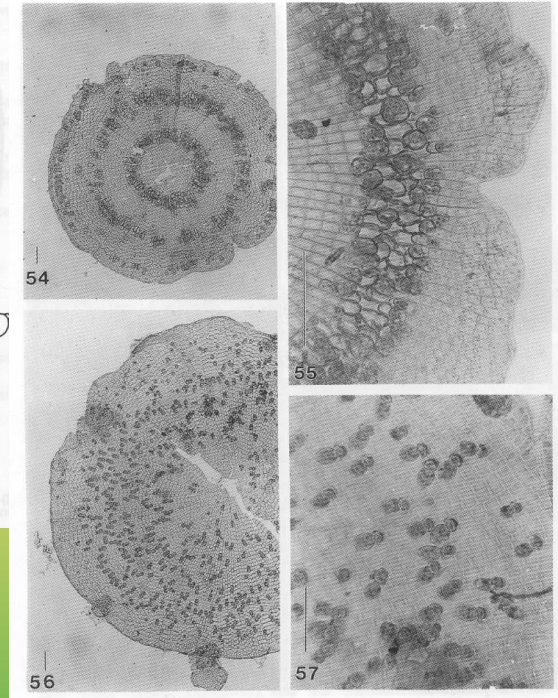
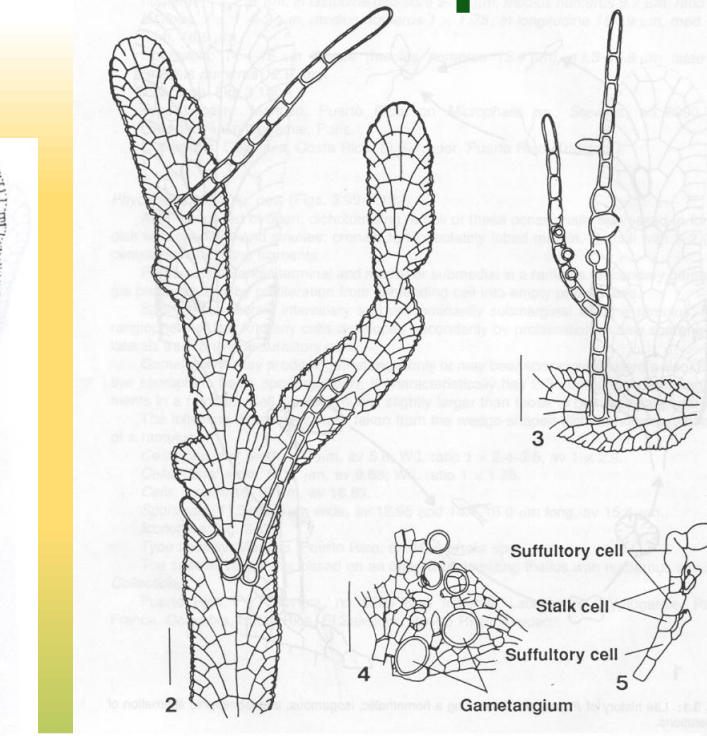
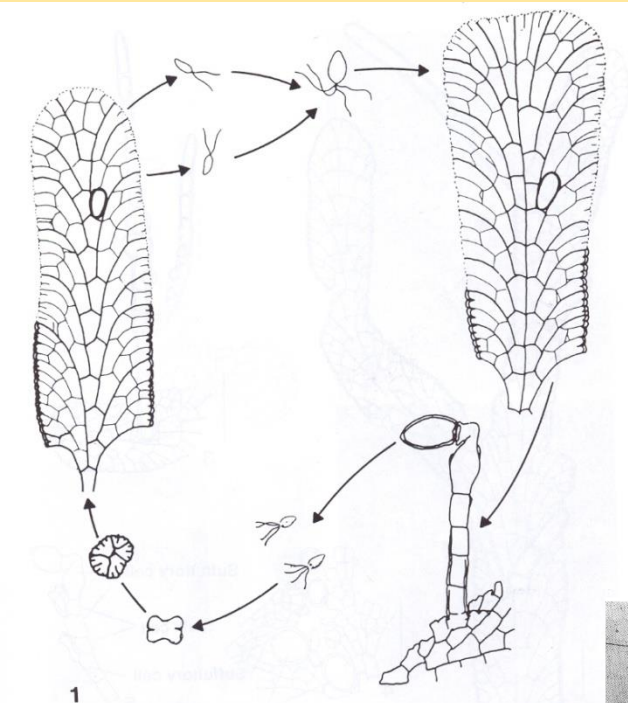


Phycopeltis



Trentepohliales – přehled rodů

Phycopeltis



Phycopeltis

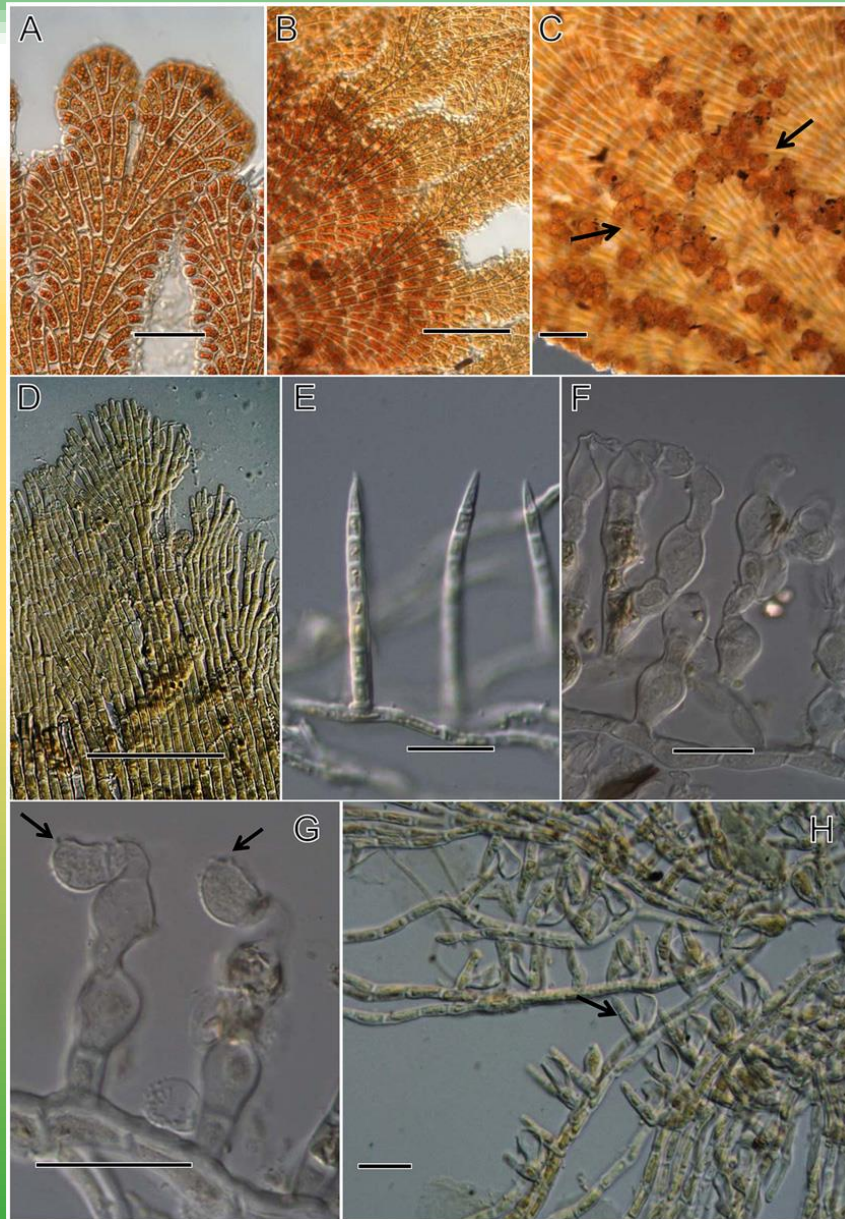
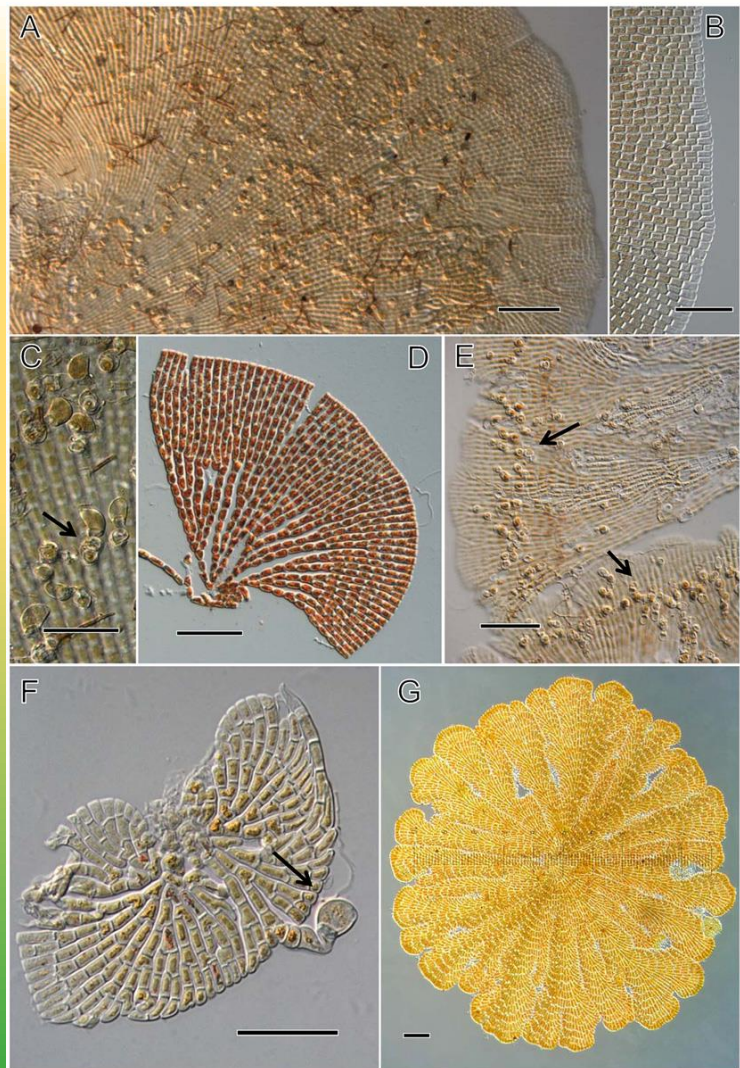


Fig 2. Microscopic features of *Phycopeltis flabellata* and *Phycopeltis prostrata*. Fig. 2A–2C. Microscopic features of *Phycopeltis flabellata*.

Bars = 50 µm. Fig. 2A. The fan-like ramuli of *P. flabellata*. Fig. 2B. New growth starting from the margins of the older ramuli. Fig. 2C. Sporangia of *P. flabellata* on the margins of fan-like ramuli. Fig. 2D–2H. Microscopic features of *Phycopeltis prostrata*. Bars for Fig. 2D, 50 µm; others, 20 µm. Fig. 2D. Disjunct margin with dichotomous filaments of *T. prostrata*. Fig. 2E. Attenuate erect hair composed of eight cells. Fig. 2F–2G. Few-celled (usually two) stalked sporangia with a terminal papilla (arrows) developing from the prostrate filaments. Fig. 2H. Sessile gametangia (arrows) on the base of erect filaments.

Zhu et al.
(2015)

Trentepohliales - přehled rodů

Cephaleuros



Fig. 1. Algal spot on avocado (*Persea americana*) caused by *Cephaleuros virescens*. Commonly called "red rust," identifying *Cephaleuros* species has confused observers for decades. Even microscopic examination of the lesions reveals hyphae-like filaments, setae, sporangiophores, and swimming spores similar to fungi and the oomycetes.

Brooks et al. (2015)

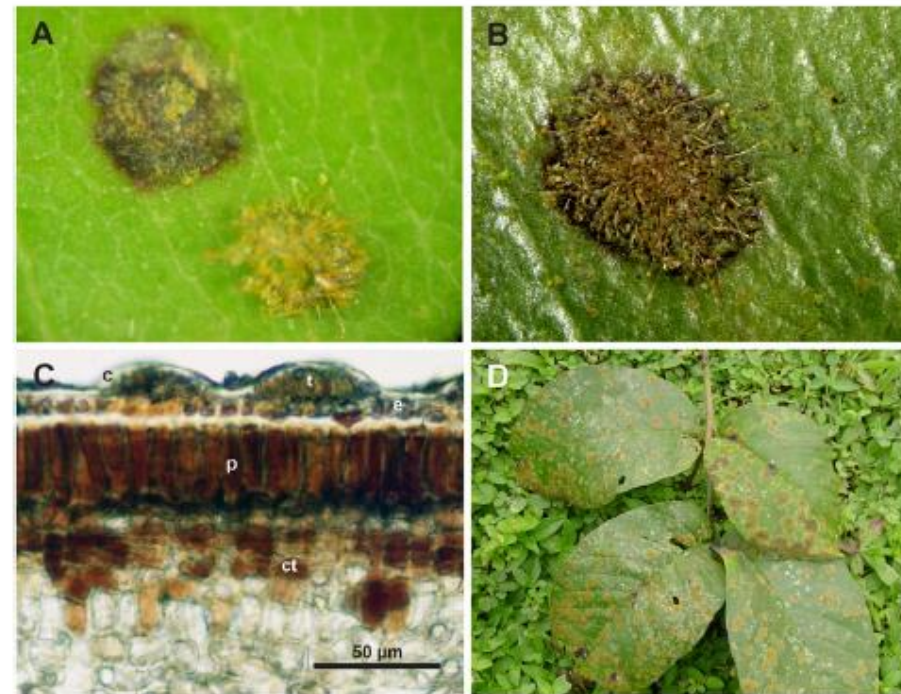


Fig. 7. **A**, Tissue necrosis caused by *Cephaleuros* species is usually limited to cells beneath the thallus. The thallus of *C. virescens* and most of the plant cuticle have been removed from the upper lesion to show necrosis. **B**, On some hosts, *Cephaleuros* causes hyperplasia of the epidermis and palisade parenchyma, raising the thallus above the leaf surface. **C**, An infection of *Camellia japonica* by the subcutaneous alga *Cephaleuros japonicus*: cuticle (c), thallus (t), epidermis (e), palisade parenchyma (p), and corky tissue (ct) formation among spongy mesophyll cells in response to infection. **D**, These yellowish orange, fuzzy thalli on guava leaves are a typical sign of *C. virescens*.

Cephaeuros

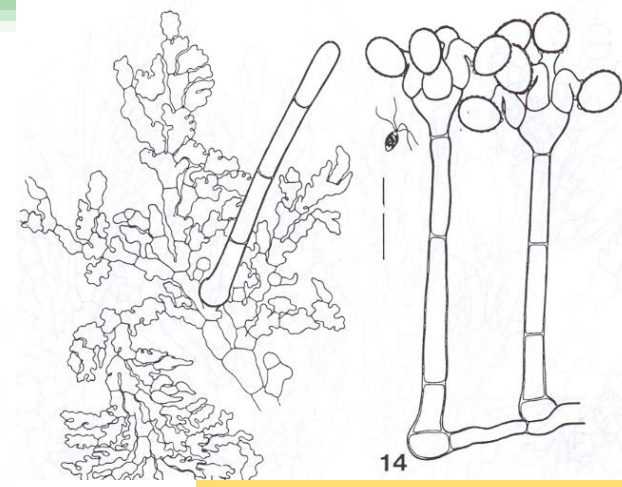
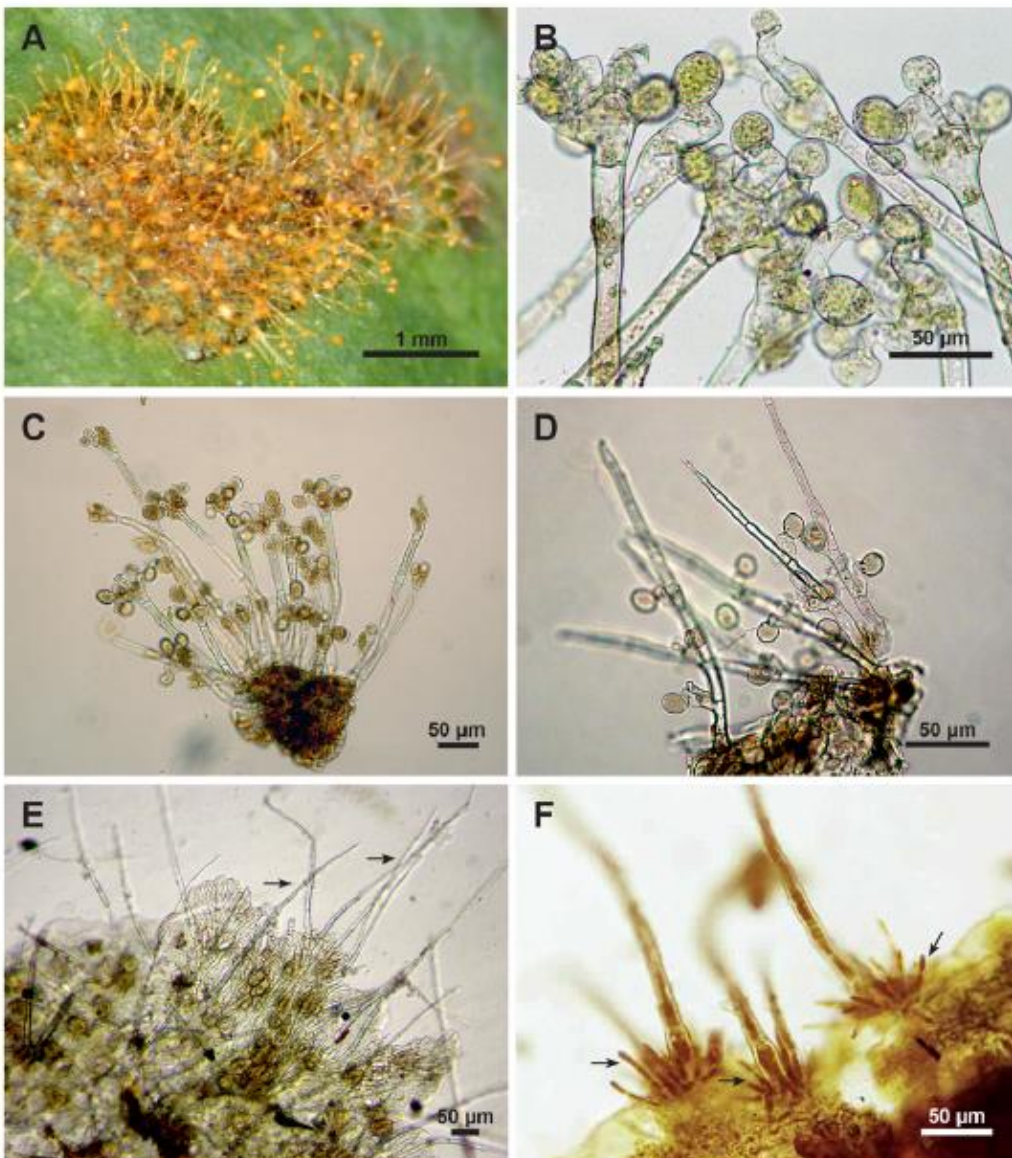
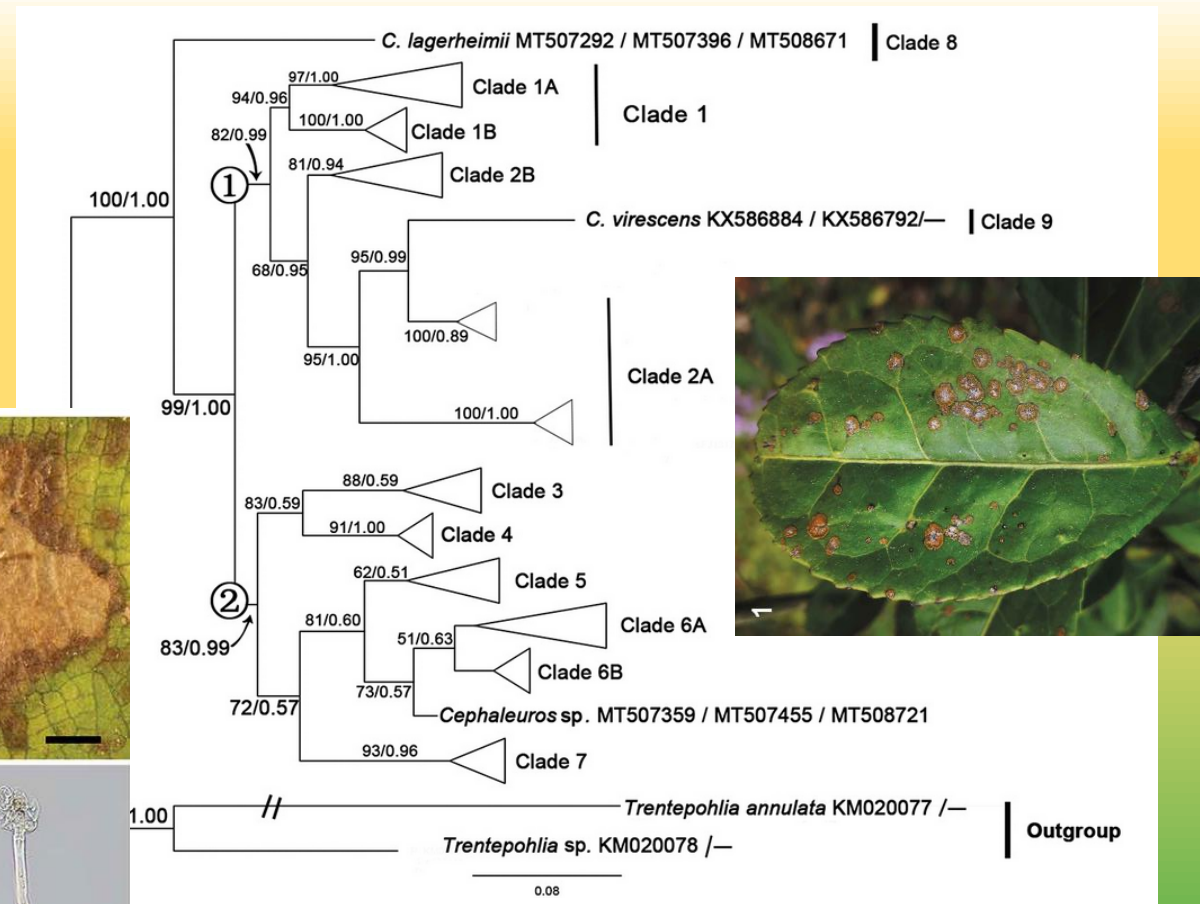
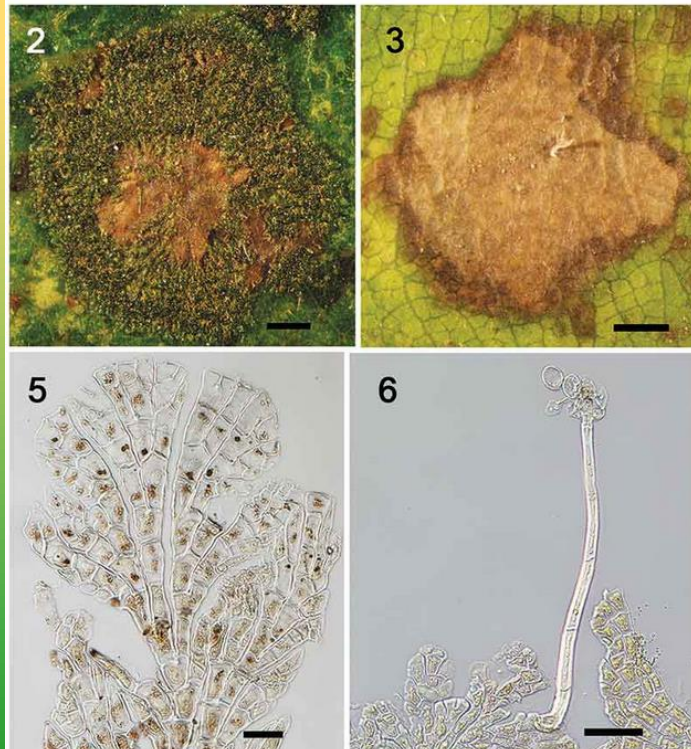


Fig. 10. When released from their gametangia and zoosporangia, gametes and zoospores both appear to have two flagella (arrows). Zoospores have four flagella, however, twisted together in two pairs. A, Gametes of *C. virescens* with two flagella (left) and zoospores with four flagella (right). B, Gametes of *C. japonicus* with two flagella (left) and zoospores with four flagella (right), both stained with Safranin O.

Fig. 9. A, Typical lesion on an upper leaf surface caused by *Cephaeuros virescens*. The erect portion of the alga consists of sporangiophores with head cells and sporangiophore-laterals, and setae. B, Head cells and sporangiophore-laterals of *C. japonicus*. C, Cluster of *C. parasiticus* sporangiophores emerging from the lower leaf surface. D, Sporangiophore-laterals of *C. minimus* form on one side of sporangiophores; the pointed, three-celled apex is sterile. E, Multicellular setae (arrows) of *C. karstenii*. F, Short setae (arrows) of *C. henningsii*.

Trentepohliales - přehled rodů

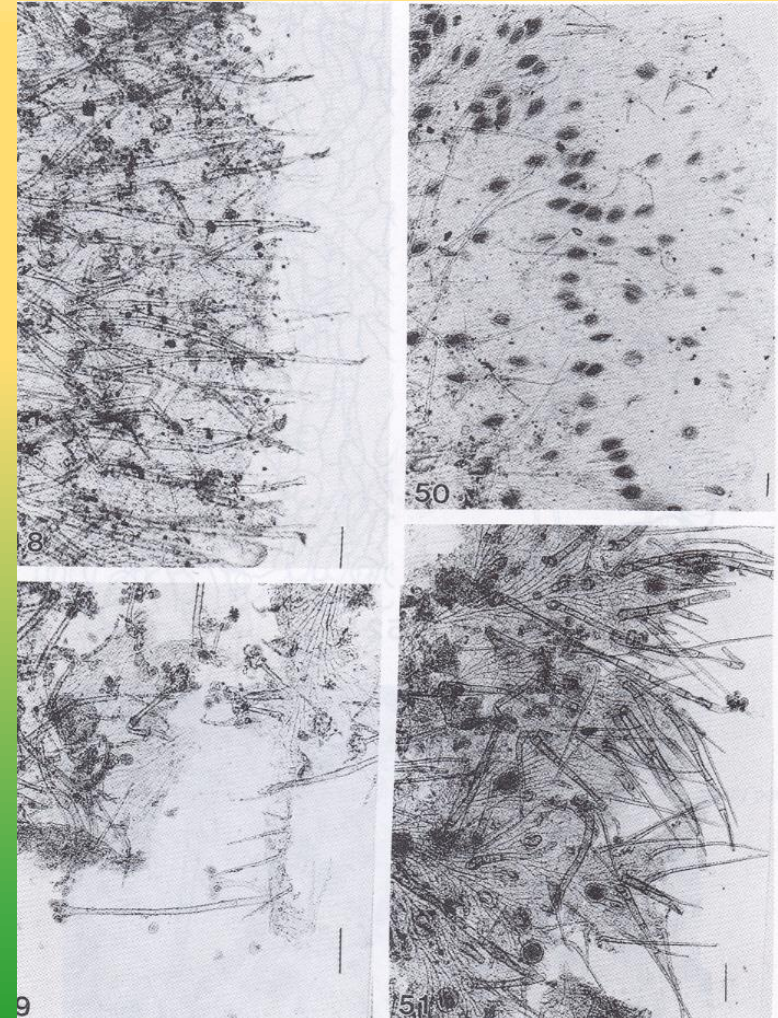
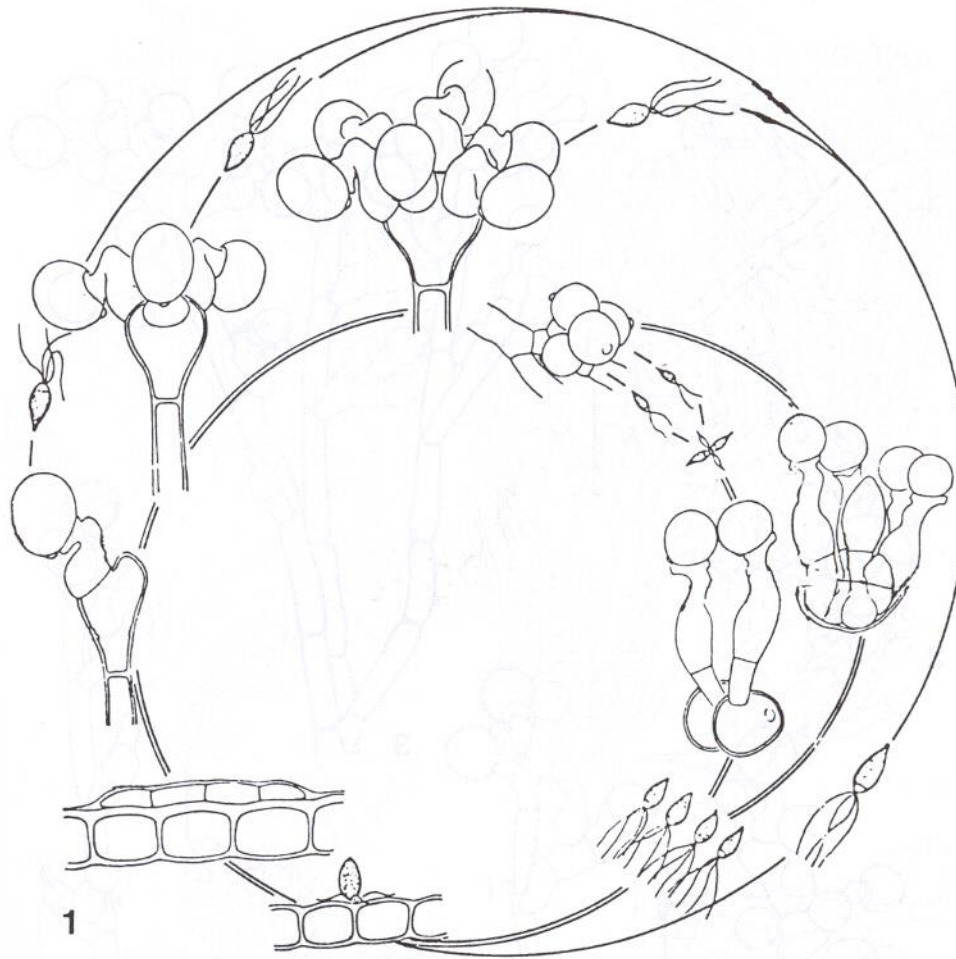
Cephaleuros



Fang et al. (2021)

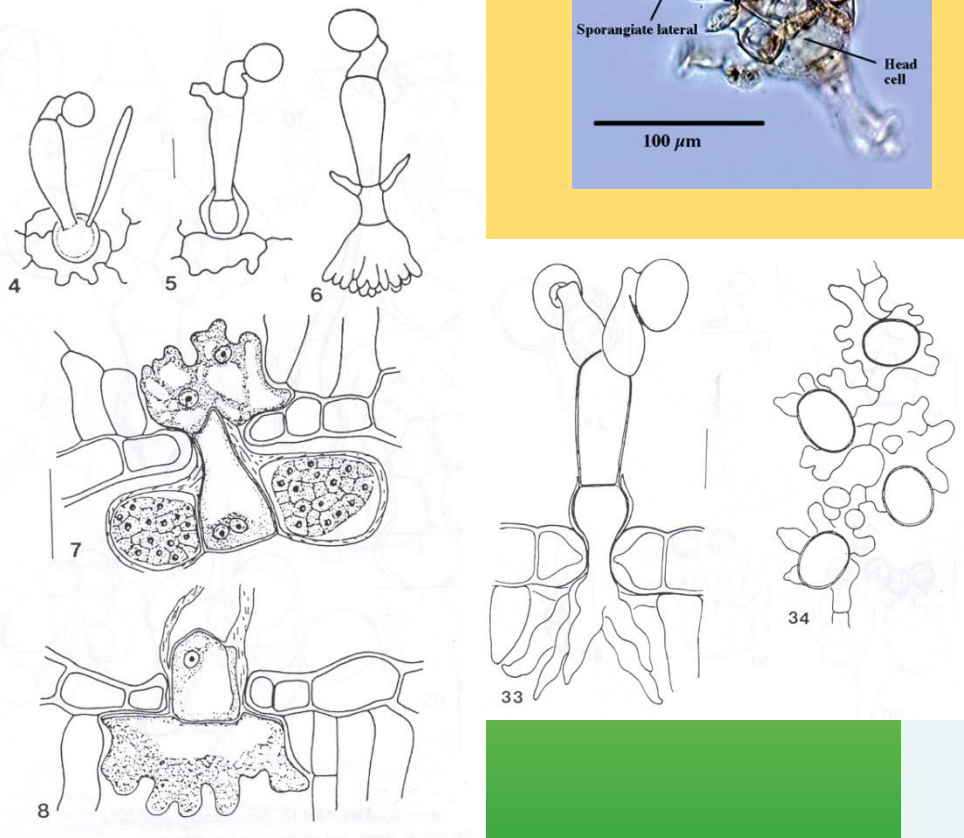
Trentepohliales - přehled rodů

Cephaleuros



Trentepohliales - přehled rodů

Stomatochroon



Zhu et al. (2014)

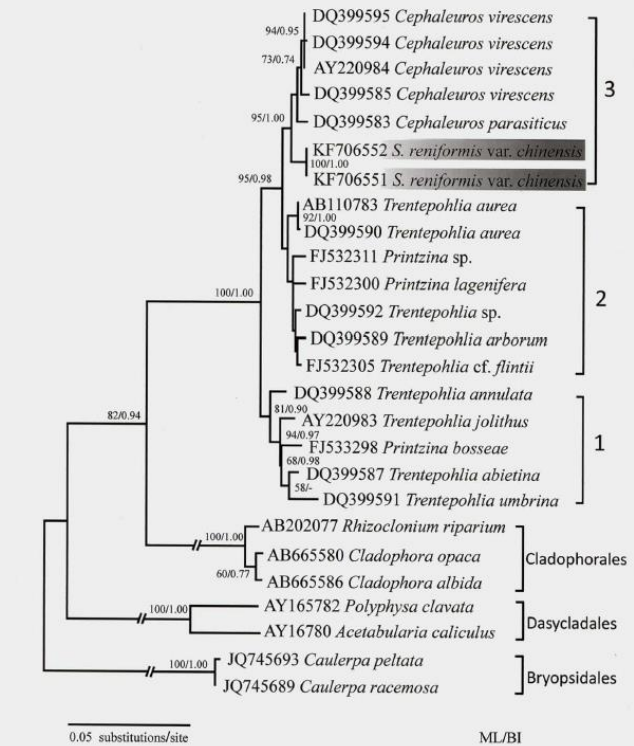
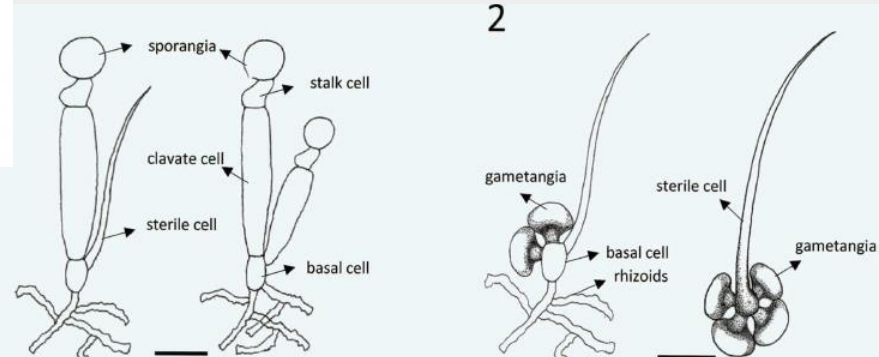


Fig. 25. Phylogram based on 18S rDNA sequences of four orders from Ulvophyceae (Trentepohliales, Cladophorales, Bryopsidales and Dasycladales). Numbers above branches are ML bootstrap support values (1000 bootstraps), and posterior probabilities from Bayesian analysis. The two strains of *Stomatochroon reniformis* var. *chinensis* are shaded in grey.



Figs 1–2. *Stomatochroon reniformis* var. *chinensis* var. nov.

Fig. 1. Line drawing showing the structure of sporophyte thalli. Scale bar = 30 μm.

Fig. 2. Line drawing showing the structure of gametophyte thalli. Scale bar = 30 μm.